ACTIVE SUSPENSION CONTROL OF TWO AXLE RAILWAY VEHICLE

MOHD.AMIR IZAT BIN MHD.RODZI

UNIVERSITI MALAYSIA PAHANG

ACTIVE SUSPENSION CONTROL OF TWO AXLE RAILWAY VEHICLE

MOHD.AMIR IZAT BIN MHD.RODZI

This thesis is submitted as partial fulfillment of the requirement for the
Award of the Bachelor Degree of Electrical Engineering (control and instrumentation)

Faculty of Electrical & Electronic Engineering
University Malaysia Pahang

NOVEMBER 2009

DECLARATION

"All the trademark and copyrights use here in are property of their respective owner. References of information from other sources are quoted accordingly, otherwise the information presented in this report is solely work of the author".

Signature : _____

Author : MOHD.AMIR IZAT BIN MHD.RODZI

Date :

DEDICATION

I specially dedicated this project to
my lovely mom and dad, my brother and my sister.

ACKNOWLEDGEMENT

I am very grateful to Allah S.W.T throughout all His Almighty kindness and loveliness for giving me the key, the strength and an opportunity to accomplish my Final Year Project.

I wish to express my sincere appreciation to my supervisor, En.Mohd.Anwar bin Zawawi for encouragement, guidance, suggestions, critics and friendship throughout achieving this project goal.

I wish to thank to other lecturers, staffs and technicians, for their cooperation, indirect or directly contribution in finishing my project. My sincere appreciation also to all my friends whose have involved and helped me in this project.

Most importantly, I wish my gratitude to my parents for their support, encouragement, understanding, sacrifice and love. For all of that, I am very thankful to the cooperation and contribution from everyone that has driven me to accomplish of this project.

ABSTRACT

This project presents the dynamic modelling and control of railway vehicle active suspension systems. Active suspension in this project concerns on the lateral movement of the railway vehicle when a curved is meet. The vehicle type selected for this study is the two-axle vehicle. The active element is place on both leading and trailing wheelset to improve the curving performance. The wheelset curving performance and vehicle body acceleration evaluated will be compared for different curve radius, cant angle, and vehicle velocity input hence the actual parameters are used for railway vehicle simulation. The optimal controller was chosen to control the lateral and yaw deflections of the two axle railway vehicle. The active suspension wheelset with two axle vehicle show different kind of performances when the curve radius, cant angle and vehicle velocity input are change.

ABSTRAK

Projek ini membincangkan model dinamik dan sistem kawalan bagi aktif suspensi bagi keretapi. Aktif suspensi dalam projek ini melibatkan pergerakan keretapi secara melintang melalui landasan keretapi yang selekoh. Jenis kenderaan yang digunakan dalam kajian ini ialah keretapi bergandar dua. Aktif elemen ditempatkan pada roda hadapan dan roda belakang untuk meningkatkan lagi prestasi selekoh. Prestasi roda sewaktu selekoh dan pecutan badan keretapi diukur akan dibandingkan untuk berlainan masukan jejari selekoh, darjah kecondongan selekoh dan kelajuan keretapi dengan parameter-parameter yang sebenar digunakan untuk simulasi keretapi. Pengawal optimum dipilih untuk mengawal anjakan melintang dan rewang bagi keretapi tersebut. Aktif suspensi dengan keretapi bergandar dua menunjukkan pelbagai prestasi apabila jejari selekoh, darjah kecondongan selekoh dan kelajuan keretapi berubah.

TABLES OF CONTENTS

CHAPTER 1

INTRODUCTION

1.1 Project Background

This project is studied on controller design and modeling the active suspension control of two axle railway vehicle in straight and curved track. The actual parameters are used in this project to get an actual performance for the two axle railway vehicle.

Different values of inputs track are use to get the feedback result from the control torque, wheelset lateral displacement, wheelset yaw angle, and vehicle body acceleration of the two axle railway vehicle base on linear state-space representation. The state-space structure was designed by using MATLAB software.

The Linear Quadratic Regulator (LQR) tuning algorithm in two axle railway vehicle model is applied to control the active suspension element. LQR consider was to be the one of the optimal type controller. An optimal control is a set of differential equations describing the paths of the control variables that minimize the cost functional.

1.2 Problem Statement

As study done here, the crucial part in railway vehicle system is the wheelset. Usually the inner side of the wheel has a large radius wheel flange compared to the outer side of the wheel. Figure 1.1 show the features of a solid-axle wheelset.

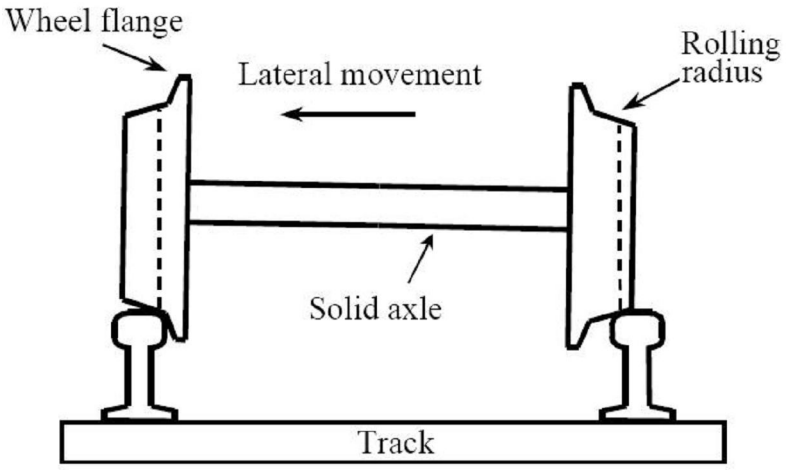

Figure 1.1: Solid-axle railway wheelset features.

When train meet a curved track corner, the wheelset and the rails have a certain consideration to make sure a good performance and safety journey of a train.

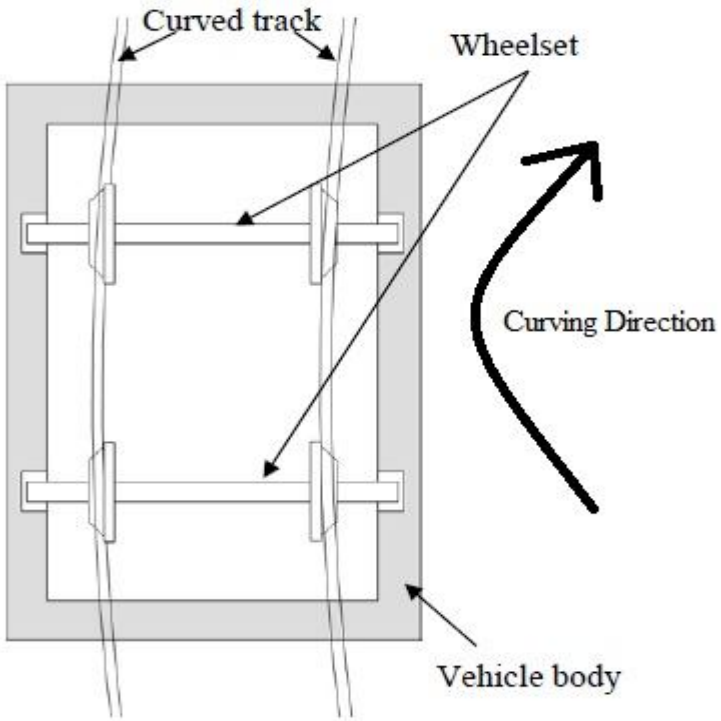

Figure 1.2: Train moving along curved track.

1.2.1 Wheelset Interaction between Rails

Wheelset interaction between rails can cause several damages to railway track. Rails also can wear out if the wheelset is not in right position. The wheelset must be in good condition which mean in good maintenance, otherwise the wheel flange is wear out. The interaction between wheelset and rails can cause loud noise.

1.2.2 Active Suspension System

Active suspension system consists of actuator, sensor and a controller. The additional elements include actuators to apply force or torque, sensors to measure and sense variable changes and feedback controller to provide control commands for the actuators.This type suspension usually requires external power to function.

Active suspension have the ability to supply and modulate the flow of energy. Thus in active suspension, many forces can be generate without depend on energy stored via spring. Some from the force created can be measure directly. The actuators at active suspension can increase the damping and thus controlling the resonance of the suspension without generating much vibration on the vehicle body.

As a summary, the potential advantages of such active suspensions are that they have low natural frequencies, which result in greater passenger comfort whilst still maintaining small static deflections, low dynamic deflections particularly under conditions of transient excitations, their suspension characteristics are maintained regardless of loading variations, high speed of response to any input and high flexibility in the choice of dynamic response especially different modes of the vehicle [1].

1.2.3 Problem Solving

i. Linear quadratic regulator is the more effective controller because it regulates the error to zero and it doesn't have percentage of overshoot and time settling. LQR also have optimal control solutions provide an automated design procedure.

ii. MATLAB is choose because it is friendly user and don't use complex coding to run it. Just drag and drop the function to use it. It also can simulate the linear system which is the linear state space equation.

1.3 Objectives

The main objective of the project is to study about the comparison of wheelset curving performance and vehicle body acceleration for different curve radius, cant angle, and vehicle velocity input by using state space modelling for two axle railway vehicle.

1.4 Scopes

In order to achieve this project, there are several scopes had been outlined:

i. Two wheelset of railway vehicle model design.
ii. Using actual parameters for railway vehicle simulation.
iii. Using modern control system which is LQR controller to control the performance.
iv. Track Input - Straight and curved track with curve radius and cant angle.
v. Use MATLAB to simulate and analyze the system performance.

1.5 Methodology

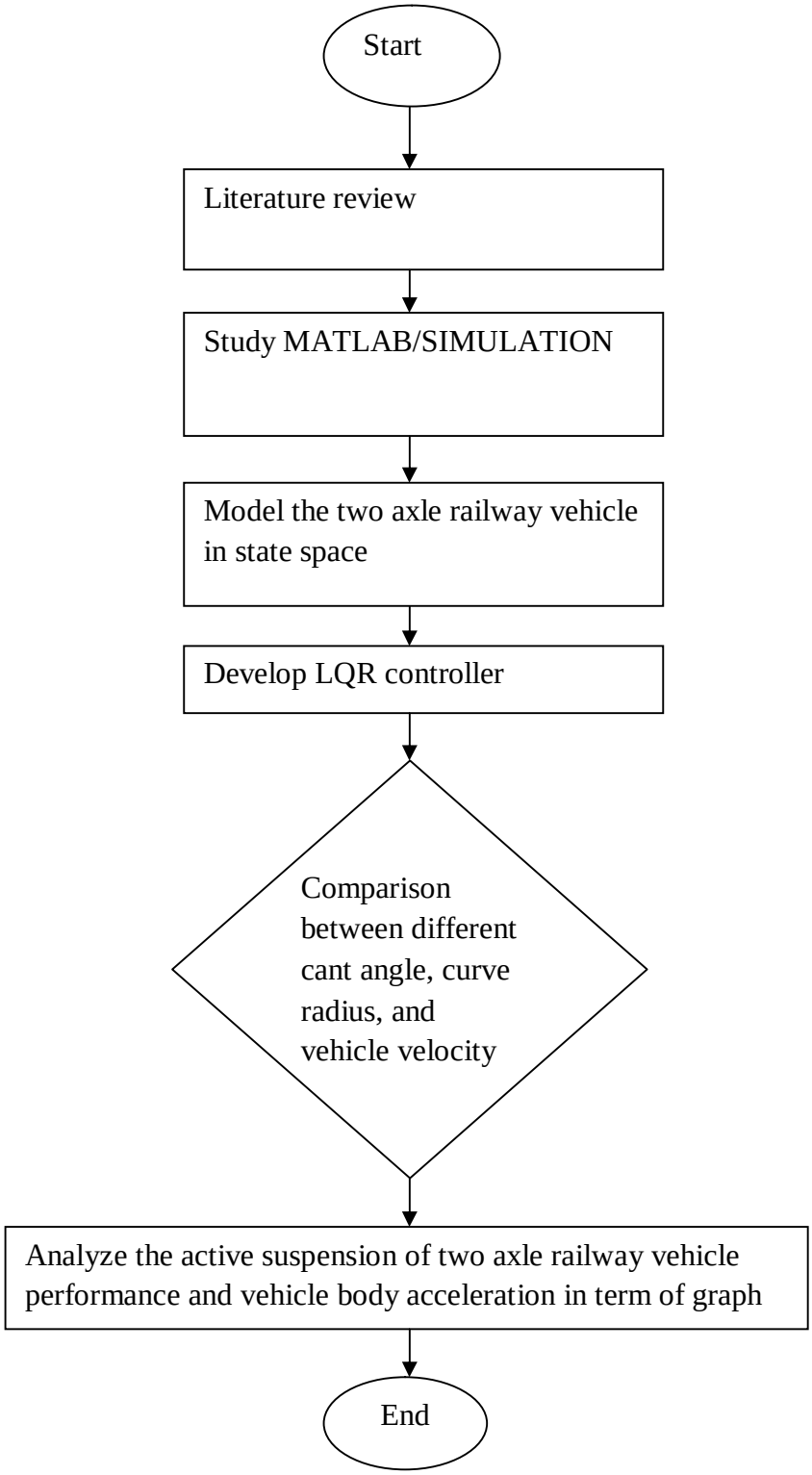

CHAPTER 2

LITERATURE REVIEW

2.1 Introduction

In this chapter include the study of linear quadratic regulator (LQR), railway vehicle which are divided into active suspension and two axle vehicle arrangement, wheelset dynamics, and railway track profile.

2.2 Linear Quadratic Regulator (LQR)

Linear quadratic regulator or LQR is commonly used technique to find the state feedback gain for a closed loop system. This is the optimal regulator, by which the open-loop poles can be relocated to get a stable system with optimal control and minimum cost for given weighting matrices of the cost function. On the other hand, by using the optimal regulator technique, that freedom of choice is lost for both discrete-time and continuous-time systems, because, in order to get a positive-definite Riccati equation solution, there are some areas where the poles cannot be assigned [10].

The problem presented by the infinite horizon LQR formulation is given a linear n-dimensional state variable system of the form: $\dot{x}(t) = Ax(t) + B\,u\,(t)$ Compute the m-dimensional control input vector u(t),

such that the performance index is minimized. Quadratic weighting matrices Q and R are selected by the designer to give appropriate state responses. It is well known that the solution is $u(t) = -Kx(t)$, where the Kalman gain, ***K,*** is given by $K = R^{-1}B^{T}P$,with ***P*** being the solution to the algebraic Riccati equation,$0 = A^{T}P + PA - PBR^{-1}B^{T}P + Q$.

The gain vector $K = R^{-1}B'P$ determines the amount of control fed back into the system. The matrix R and Q, will balance the relative importance of the control input and state in the cost function (J) being optimized with a condition that the elements in both Q and R matrices are positive values. The size of Q matrix depends on the size of the system's state matrix and R matrix is dependent on the number of control input to the system [11].

Using MATLAB, the algebraic Ricatti equation is solved and the control gain K is evaluated for different values of Q and R weighting matrices. The response of the system is simulated as well. The weighting matrix R is a scalar value as there is only one control input to the system. The values in the Q matrix are adjusted according to the required response of the system; a higher value of the weightings indicates the importance of the states [12].

2.3 Railway Vehicle

2.3.1 Active Suspension

Active suspension systems dynamically respond to changes in the rail track profile because of their ability to supply energy that can be used to produce relative motion between the body and wheel. Typically, active suspension systems include sensors to measure suspension variables such as body velocity, suspension displacement, wheel velocity and wheel or body acceleration. An active suspension is one in which the passive components are augmented by actuators that supply

additional forces. These additional forces are determined by a feedback control law using data from sensors attached to the vehicle [3].

The key characteristic of the active suspension system is that an external power source is used to achieve the desired suspension goal. The actuator is placed as a secondary suspension system for the vehicle. The controller drives actuator based on the designed control law. The active suspension system provides the freedom to adjust the entire suspension system, and the control force can be introduced locally or globally based on the system state [2].

2.3.2 Two-Axle Vehicle Arrangement

In this study, two wheel sets railway vehicle consists of torque actuator, two wheel sets, lateral suspension and vehicle body is used. The arrangement of two wheel sets is shown in Figure 2.1 [9].

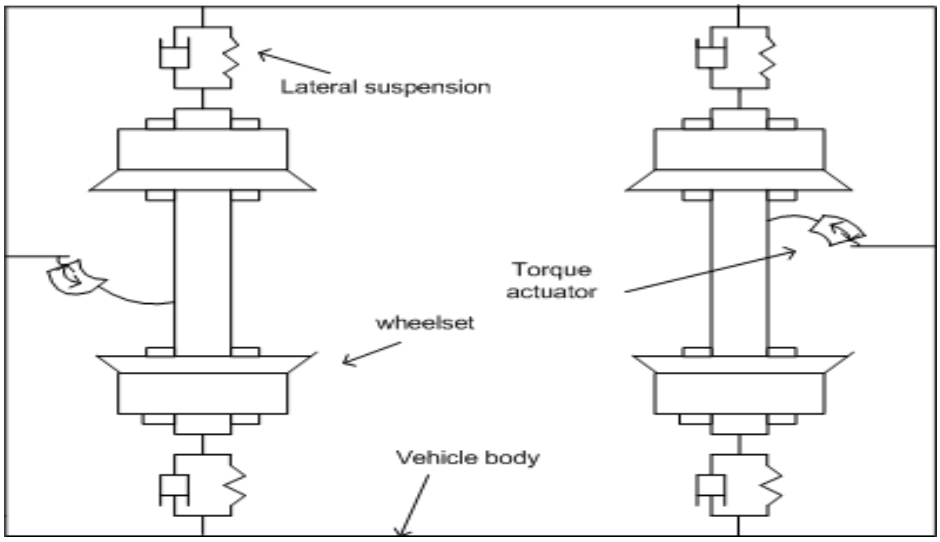

Figure 2.1: Two axle arrangement figure.

2.4 Wheelset General Equation

In general, the lateral and yaw displacement of a single wheelset are depending on creep damping and creep stiffness of the wheelset. Due to the lateral displacement, the wheelset interactions with the rails can cause damages to the track, wear of rails, wear of wheel flange, and noise in the contact area [4].

For a single wheelset, the second-order differential equations that represent the relationship of creep damping and creep stiffness coefficient with lateral and yaw displacement can been shown below:

$$\ddot{y} = \frac{-2f_{11}}{mV}\dot{y} + \frac{-2f_{22}}{m}\psi + \frac{1}{m}F_y \tag{2.1}$$

$$\ddot{\psi} = \frac{-2f_{11}l\lambda}{I_w r}y - \frac{-2f_{11}l^2}{I_w V}\dot{\psi} + \frac{1}{I_w}T_w \tag{2.2}$$

where;

y is the lateral displacement of the wheelset
ψ is the yaw angle (angle of attack)
F_y is the external lateral force
T_ψ is the external yaw torque
m is the mass of the wheelset
I_w is the moment of inertia of the wheelset
f_{11} is the longitudinal creep coefficient of the wheelset
f_{22} is the lateral creep coefficient of the wheelset

2.5 Railway Track Profile

2.5.1 Curve Radius and Cant Angle

To study the suspension curving performance, the input of the system has to be a curved track with a certain radius and corresponding cant angle (a deterministic track input). In this research, the curved track is connected to straight tracks on either end via one second time transition. The time transition is necessary to reduce the curving effects on the vehicle's passenger. The curved track is canted inwards to reduce the lateral acceleration experienced by the passengers [5]. The vehicle speed (e.g. balance speed) on curved track can be determined from the following balance equation:

$$V_{bal}=\sqrt{R\times g\times\tan\theta_c} \tag{2.3}$$

where;

V_{bal} is the balance speed (ms^{-1})
R is the curve radius (m)
g is the gravity ($9.81\,ms^{-2}$)
θ_c is the cant angle (deg.)

In this study, the curve radius is 1500 m and the cant angle is 14^o. This will give the balance speed at curved track equal to 60.6 ms^{-1}. As the vehicle is required to run at a higher speed level (e.g. 60 ms^{-1}), the cant deficiency standard has to be fulfilled for safety purposes.

2.5.2 Cant Deficiency

Cant is defined as the elevation of the outside rail minus the elevation of the inside rail of a curved track (synonym to the superelevation of the curve). Cant deficiency presents when a vehicle's speed on a curve is greater than the speed (e.g. *balance speed*) at which the components of wheel to rail force normal to the plane of the track would be the same in aggregate for the outside rails as for the inside rails. For a railway vehicle that travels at a higher speed than the balancing speed, the cant deficiency is given as follow:

$$CD = \frac{g_r}{\sqrt{1+\frac{R^2 g^2}{V^4}}} - SE \tag{2.4}$$

where;

CD is cant deficiency (mm)
g is the gravity
g_r is the rail gauge (mm)
R is the curve radius
SE is the superelevation of the track (mm)
V is the vehicle speed (ms^{-1})

According to the standard gauge railroads in the United States, the superelevation is limited to eight inches (8”) or equal to 203.2 mm [6]. As for the rail gauge, the standard value is 1435 mm [7]. The standard value for cant deficiency is different between countries, and it is depending on the type of the vehicle (tilting or non-tilting trains) [8]. In this study, the maximum allowable cant deficiency is referred to the United States standard for non-tilting trains which is seven inches (7”) or equal to 177.8 mm.

CHAPTER 3

DYNAMIC MODELING

3.1 Introduction

In this chapter, the characteristics of a solid axle wheelset and mathematical modeling for two axle wheelset are presented.

3.2 Solid Axle Wheelset Characteristics

In today world, usually the solid axle wheelset was chosen because it offers a lot of advantages. There are two types of solid axle wheelset which are conical wheelset and profiled as shown in Figure 3.1 and Figure 3.2. For this study, the highlight for the solid axle wheelset characteristics were natural curving, perfect curving, wheelset hunting and mathematical description including state space representation.

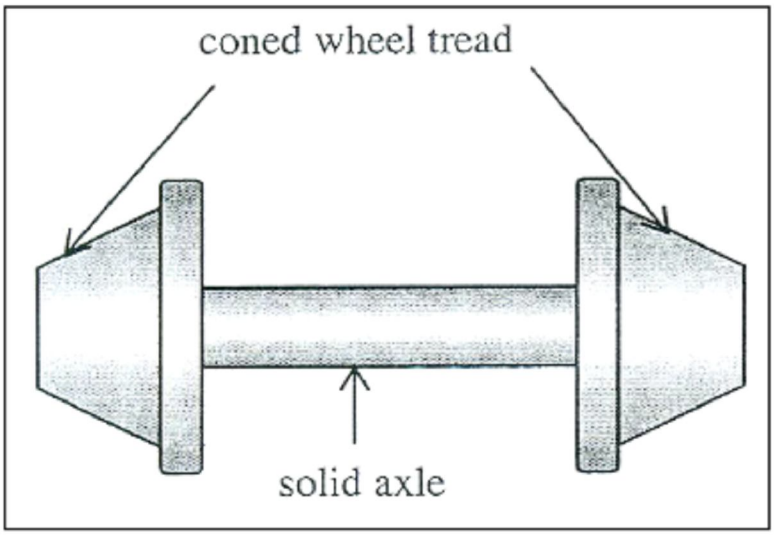

Figure 3.1: Conical Wheelset

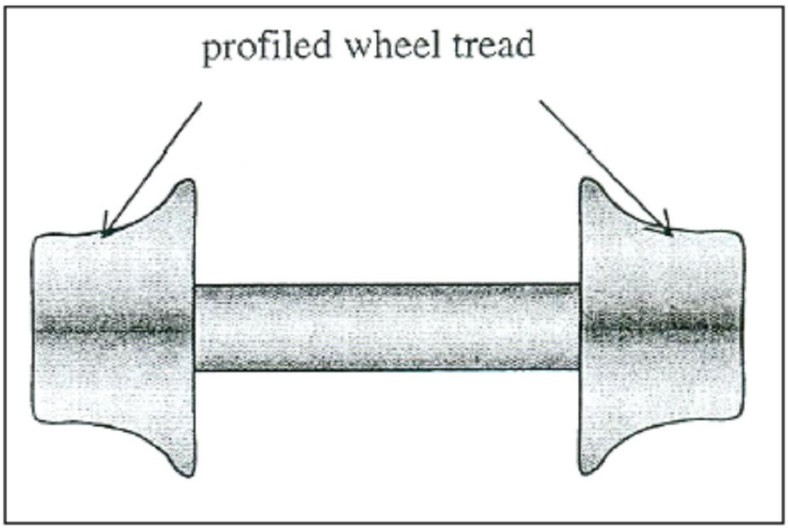

Figure 3.2: Profiled Wheelset

3.2.1 Natural Curving

The solid-axle wheelset is a combination of two coned/profiled wheels that are rigidly connected to a common axle. The wheels must rotate at the same rotational speed, same as the outer wheel moves faster along the track, and the effect is to make the wheelset go around the curve. Some misconception is that, it is the flange which makes the vehicle follows the curve. But in fact, it is entirely a result of the profiling of the wheels. This advantage of following the rail track particularly on curved track is also known as ‘natural curving’.

3.2.2 Perfect Curving

When the railway vehicle moves along a curved track, the wheelsets tend to move inside of the curve radius laterally besides experiencing the cant angle displacement at the same time. To get a pure rolling action (the perfect curving), it is necessary to choose a good control scheme to enhance the curving performance of the vehicle suspension system.

3.2.3 Wheelset Hunting

Because the wheels are connected together to a common axle, this wheelset is also inherently unstable at any non-zero speed and it exhibits a sustained oscillation in the lateral ground or known as ‘wheelset hunting’. Figure 3.3 shows the wheelset moves in sinusoidal direction due to the characteristics of the wheelset.

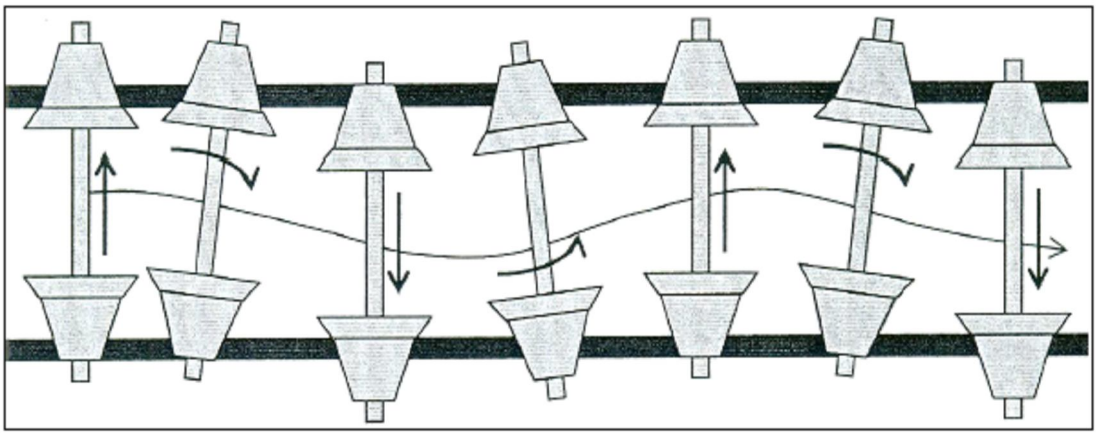

Figure 3.3: Wheelset Hunting

3.2.4 Mathematical Description

The complete equations of linear model of a single solid axle wheelset travelling on a straight track with lateral irregularities are given in Equations (3.1) and (3.2) below [13]:

$$m\ddot{y}_w = \frac{-2f_{11}}{V}\dot{y}_w + 2f_{22}\psi_w + F_y \tag{3.1}$$

$$I_w\ddot{\psi}_w = \frac{-2f_{11}l\lambda}{r}y_w - \frac{-2f_{11}l^2}{V}\dot{\psi}_w + T_\psi \tag{3.2}$$

3.2.5 State-Space Representation

The differential equations in equations (3.1) and (3.2) are represented in state space form as below:

$$\dot{x} = A_w x + B_w u \tag{3.3.1}$$

$$y = C_w x + D_w u \tag{3.3.2}$$

where;

$$x = \begin{bmatrix} x_1 & x_2 & x_3 & x_4 \end{bmatrix}^T = \begin{bmatrix} \dot{y}_w & y_w & \dot{\psi}_w & \psi_w \end{bmatrix}^T \tag{3.3.3}$$

$$\dot{x} = \begin{bmatrix} \dot{x}_1 & \dot{x}_2 & \dot{x}_3 & \dot{x}_4 \end{bmatrix}^T = \begin{bmatrix} \ddot{y}_w & \dot{y}_w & \ddot{\psi}_w & \dot{\psi}_w \end{bmatrix}^T \tag{3.3.4}$$

$$u = \begin{bmatrix} F_y & T_\psi \end{bmatrix}^T \tag{3.3.5}$$

and the system matrix (*Aw*), input matrix (*Bw*), output matrix (*Cw*) and feedforward matrix (*Dw*) as below:

$$A_w = \begin{bmatrix} \frac{-2 f_{22}}{mV} & 0 & 0 & \frac{2 f_{22}}{m} \\ 1 & 0 & 0 & 0 \\ 0 & \frac{-2 f_{11} l \lambda}{I_\psi r} & \frac{-2 f_{11} l^2}{I_\psi V} & 0 \\ 0 & 0 & 1 & 0 \end{bmatrix} \tag{3.3.6}$$

$$B_w = \begin{bmatrix} \frac{1}{m} & 0 \\ 0 & 0 \\ 0 & \frac{1}{I_\psi} \\ 0 & 0 \end{bmatrix} \tag{3.3.7}$$

$$C_w = \begin{bmatrix} 0 & 1 & 0 & 0 \\ 0 & 0 & 0 & 1 \end{bmatrix} \tag{3.3.8}$$

$$D_w = \begin{bmatrix} 0 & 0 \\ 0 & 0 \end{bmatrix} \tag{3.3.9}$$

3.3 Two-Axle Railway Vehicle

3.3.1 Mathematical Description

For the two axle railway vehicle system mathematical equations can be extended from equations (3.1) and (3.2) that represent the dynamic characteristics of a single solid axle wheelset. By adding another solid axle wheelset and a vehicle body into the previous single solid axle wheelset, the mathematical description of the two axle vehicle can be determined as below:

i. Leading wheelset:

$$m\ddot{y}_{w1} = \left[\frac{-2f_{11}}{V} - C_w\right]\dot{y}_{w1} - K_w y_{w1} + 2f_{22}\psi_{w1} + C_w\dot{y}_v + K_w y_v + C_w l_b\dot{\psi}_v + K_w l_b\psi_v \quad (3.4.1)$$

$$I_w\ddot{\psi}_{w1} = \frac{-2f_{11}l\lambda}{r}y_{w1} - \frac{2f_{11}l^2}{V}\dot{\psi}_{w1} + T_{\psi 1} \quad (3.4.2)$$

ii. Trailing wheelset:

$$m\ddot{y}_{w2} = \left[\frac{-2f_{11}}{V} - C_w\right]\dot{y}_{w2} - K_w y_{w2} + 2f_{22}\psi_{w2} + C_w\dot{y}_v + K_w y_v - C_w l_b\dot{\psi}_v - K_w l_b\psi_v \quad (3.4.3)$$

$$I_w\ddot{\psi}_{w2} = \frac{-2f_{11}l\lambda}{r}y_{w2} - \frac{2f_{11}l^2}{V}\dot{\psi}_{w2} + T_{\psi 2} \quad (3.4.4)$$

iii. Vehicle body:

$$m\ddot{y}_v = C_w\dot{y}_{w1} + K_w y_{w1} + C_w\dot{y}_{w2} + K_w y_{w2} - 2C_w\dot{y}_v - 2K_w y_v \quad (3.4.5)$$

$$I_v\ddot{\psi}_v = C_w l_b\dot{y}_{w1} + K_w l_b y_{w1} - C_w l_b\dot{y}_{w2} - K_w l_b y_{w2} - 2C_w l_b^2\dot{\psi}_v - 2K_w l_b^2\psi_v - T_{\psi 1} - T_{\psi 2} \quad (3.4.6)$$

3.3.2 State-Space Representation

The dynamic equations of two axle railway vehicle are similar to the ones for solid axle wheelset. But, instead of only having system matrix, input matrix and output matrix, the state equation of two axle vehicle has another matrix component to describe the deterministic track input into the system; curve radius and cant angle. The standard state equation in equation (3.3.1) is modified as below [14]:

$$\dot{x} = A_a x + B_a u + G_a w \tag{3.5.1}$$

where;

$$x = \begin{bmatrix} \dot{y}_{w1} & y_{w1} & \dot{\psi}_{w1} & \psi_{w1} & \dot{y}_{w2} & y_{w2} & \dot{\psi}_{w2} & \psi_{w2} & \dot{y}_v & y_v & \dot{\psi}_v & \psi_v \end{bmatrix}^T \tag{3.5.2}$$

$$\dot{x} = \begin{bmatrix} \ddot{y}_{w1} & \dot{y}_{w1} & \ddot{\psi}_{w1} & \dot{\psi}_{w1} & \ddot{y}_{w2} & \dot{y}_{w2} & \ddot{\psi}_{w2} & \dot{\psi}_{w2} & \ddot{y}_v & \dot{y}_v & \ddot{\psi}_v & \dot{\psi}_v \end{bmatrix}^T \tag{3.5.3}$$

$$u = \begin{bmatrix} T_{\psi 1} & T_{\psi 2} \end{bmatrix}^T \tag{3.5.4}$$

$$w = \begin{bmatrix} 1/R_1 & \theta_{c1} & 1/R_2 & \theta_{c2} \end{bmatrix}^T \tag{3.5.5}$$

and system matrix *Aa* is given below:

(3.5.6)

$$A_a = \begin{bmatrix} a_{1,1} & a_{1,2} & 0 & a_{1,4} & 0 & 0 & 0 & 0 & a_{1,9} & a_{1,10} & a_{1,11} & a_{1,12} \\ 1 & 0 & 0 & 0 & 0 & 0 & 0 & 0 & 0 & 0 & 0 & 0 \\ 0 & a_{3,2} & a_{3,3} & 0 & 0 & 0 & 0 & 0 & 0 & 0 & 0 & 0 \\ 0 & 0 & 1 & 0 & 0 & 0 & 0 & 0 & 0 & 0 & 0 & 0 \\ 0 & 0 & 0 & 0 & a_{5,5} & a_{5,6} & 0 & a_{5,8} & a_{5,9} & a_{5,10} & a_{5,11} & a_{5,12} \\ 0 & 0 & 0 & 0 & 1 & 0 & 0 & 0 & 0 & 0 & 0 & 0 \\ 0 & 0 & 0 & 0 & 0 & a_{7,6} & a_{7,7} & 0 & 0 & 0 & 0 & 0 \\ 0 & 0 & 0 & 0 & 0 & 0 & 1 & 0 & 0 & 0 & 0 & 0 \\ a_{9,1} & a_{9,2} & 0 & 0 & a_{9,5} & a_{9,6} & 0 & 0 & a_{9,9} & a_{9,10} & 0 & 0 \\ 0 & 0 & 0 & 0 & 0 & 0 & 0 & 0 & 1 & 0 & 0 & 0 \\ a_{11,1} & a_{11,2} & 0 & 0 & a_{11,5} & a_{11,6} & 0 & 0 & 0 & 0 & a_{11,11} & a_{11,12} \\ 0 & 0 & 0 & 0 & 0 & 0 & 0 & 0 & 0 & 0 & 1 & 0 \end{bmatrix}$$

where;

$a_{1,1}$ and $a_{5,5} = \left[-\frac{2f_{22}}{mV} - \frac{C_w}{m} \right]$

$a_{1,2}$ and $a_{5,6} = -\frac{K_w}{m}$

$a_{1,4}$ and $a_{5,8} = \frac{2f_{22}}{m}$

$a_{1,9}$ and $a_{5,9} = \frac{C_w}{m}$

$a_{1,10}$ and $a_{5,10} = \frac{K_w}{m}$

$a_{1,11}$ and $-a_{5,11} = \frac{C_w l_b}{m}$

$a_{1,12}$ and $-a_{5,12} = \frac{K_w l_b}{m}$

$a_{3,2}$ and $a_{7,6} = \frac{-2f_{11} l\lambda}{I_w r}$

$a_{3,3}$ and $a_{7,7} = \frac{-2f_{11} l^2}{I_w V}$

$a_{9,1}$ and $a_{9,5} = \frac{C_w}{m_v}$

$a_{9,2}$ and $a_{9,6} = \frac{K_w}{m_v}$

$a_{9,9} = \frac{-2C_w}{m_v}$

$a_{9,10} = \frac{-2K_w}{m_v}$

$a_{11,1}$ and $-a_{11,5} = \frac{C_w l_b}{I_V}$

$a_{11,2}$ and $-a_{11,6} = \frac{K_w l_b}{I_v}$

$a_{11,11} = \frac{-2C_w l_b^2}{I_v}$

$a_{11,12} = \frac{-2K_w l_b^2}{I_v}$

and input matrix, *Ba* is:

$$B_a = \begin{bmatrix} 0 & 0 \\ 0 & 0 \\ 1/I_w & 0 \\ 0 & 0 \\ 0 & 0 \\ 0 & 0 \\ 0 & 1/I_w \\ 0 & 0 \\ 0 & 0 \\ 0 & 0 \\ -1/I_v & -1/I_v \\ 0 & 0 \end{bmatrix} \tag{3.5.7}$$

and finally disturbance matrix, *Ga* is:

$$G_a = \begin{bmatrix} V^2 & -g & 0 & 0 \\ 0 & 0 & 0 & 0 \\ \frac{2f_{11}l^2}{I_w} & 0 & 0 & 0 \\ 0 & 0 & 0 & 0 \\ 0 & 0 & V^2 & -g \\ 0 & 0 & 0 & 0 \\ 0 & 0 & \frac{2f_{11}l^2}{I_w} & 0 \\ 0 & 0 & 0 & 0 \\ \frac{V^2}{2} & \frac{g}{2} & \frac{V^2}{2} & \frac{g}{2} \\ 0 & 0 & 0 & 0 \\ 0 & 0 & 0 & 0 \\ 0 & 0 & 0 & 0 \end{bmatrix} \tag{3.5.8}$$

3.3.3 Vehicle Parameter Values For Simulation

The parameters values for two axle vehicle simulation are referred to [14] as shown in Table 3.1 below:

Table 3.1: Two-axle Railway Vehicle Parameters Symbol

Symbol	Description	Value
y_{w1}, y_{w2} , y_v	Lateral displacement of front, middle, rear wheelset and body	-
ψ_{w1}, ψ_{w2}, ψ_v	Yaw displacement of front, middle, rear and body	-
V	Vehicle velocity	60 m/s, 80m/s, 100m/s
m, m_v	Wheelset and vehicle mass	1250 kg 13500 kg
I_w I_v	Wheelset and vehicle inertia	700 kgm^2 17x10^4 kgm^2
l_b	Half spacing between two wheelset	3.7 m
K_w	Lateral stiffness per wheelset	230 kN/m
C_w	Lateral stiffness per wheelset	50 kN s/m
r	Wheel radius	0.45 m
λ	Conicity	0.2
l	Half gauge of wheelset	0.7 m
f_{11}	Longitudinal creep coefficient	10 MN
f_{22}	Lateral creep coefficient	10 MN
R_1, R_2	Radius of the curved track at the front and rear wheelsets	1000 m, 1500 m, 2000 m
θ_1, θ_2	Cant angle of the curved track at the front and rear wheelsets	7^o, 14^o, 21^o
$T_{\psi 1}$, $T_{\psi 2}$	Controlled torque input for front and rear wheelsets	-
g	Gravity	9.8 m/s^2

CHAPTER 4

CONTROLLER DESIGN

4.1 Introduction

For this chapter, the controller type used in the two-axle railway vehicle models. For the two-axle vehicle, the dynamic characteristics consists of 12 states that represent the lateral and yaw displacement as well as its corresponding velocities for each of the two wheelsets and vehicle body. Thus, it is too complex and difficult to use classical control approach to deal with such high order system. As a solution, modern control approach that can handle the state space of high order system is highly desired.

4.2 Control Structure

The most important part in choosen the right controller are the controller must stabilize the system and the closed loop system should be robust against variation of operational parameters such as wheel conicity and creepage coefficients. Secondly, the controller to be designed should not interfere with the natural curving action of the wheelsets.

General diagram of the control structure is provided in Figure 4.1 [15]. The input of the system is the track input (deterministic input) which the curve radius and the cant angle are predetermined according to the standard provided by responsible bodies.

The system information consists of system matrix, input matrix, output matrix and disturbance matrix (in state space representation). Sensors are applied to sense appropriate parameters to be measured and feedback into the system. Actuators are used to give any physical changes towards the controlled system. The actuator type can be either hydraulic, pneumatic, motor driven or combination between them.

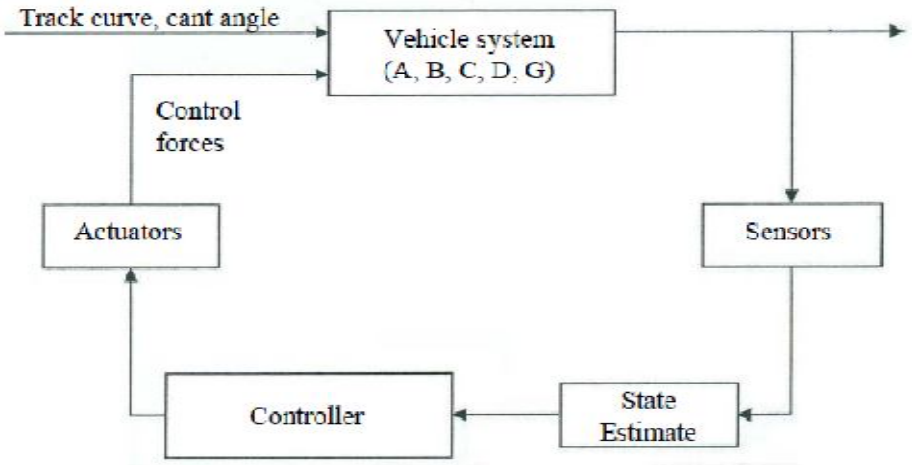

Figure 4.1: Control Structure Diagram

4.3 Linear Quadratic Regulator

Optimal control is concerned with operating a dynamic system at minimum cost. Linear quadratic regulator (LQR) is the case where the system dynamics are described by a set of linear differential equations and the cost, *J* is described by a quadratic functional.

The settings of the LQR controller are found by using a mathematical algorithm that minimizes the cost function with weighting factors determined by the controller designer (human). The cost function is often defined as a sum of the deviations of key measurements from their desired values. In effect, this algorithm will then find those controller settings that minimize the undesired deviations.

The LQR algorithm takes care of the tedious work to optimizing the controller. However, the controller designer still needs to specify the weighting factors and compare the results with the specified design goals. As a result, controller

synthesis will still be an iterative process where the designer judges the designed optimal controllers through simulation and then adjusts the weighting factors to get a controller more in line with the specified design goals.

When designing an optimal controller, the system is assumed to be linear and has a state equation in the form below:

$$\dot{x} = Ax + Bu \tag{4.1}$$

$$y = Cx \tag{4.2}$$

the control law is chosen such that it minimizes the cost function;

$$J = \int \left(y^T(t) \cdot Q \cdot y(t) + u^T(t) \cdot R \cdot u(t) \right) dt \tag{4.3}$$

where y represents the selected states to be controlled. In this simulation study for two-axle vehicle, y is described as below:

$$y = \begin{bmatrix} y_{w1} & \theta_{w1} & y_{w2} & \theta_{w2} \end{bmatrix}^T \tag{4.4}$$

As for the weighting matrices, Q and R are important to get a perfect optimal controller. In this study, R is fixed at 10^{-12} to maintain a good tracking performance and Q is to be adjusted. After several attempts, the appropriate values of Q for two-axle vehicle are determined and shown below:

$$Q = diag \begin{bmatrix} 100 & 10 & 100 & 10 \end{bmatrix} \tag{4.5}$$

$$R = diag \begin{bmatrix} 10^{-12} & 10^{-12} \end{bmatrix} \tag{4.6}$$

The control law is given Equation 5.6 below [16]:

$$u(t) = -K(t)\, x(t) \tag{4.7}$$

The feedback gain matrix *K* is described below:

$$K(t) = -R^{-1}B^{T}(t)P_{r}(t) \tag{4.8}$$

and *Pr* is obtained by solving Ricatti equation below:

$$\dot{P}_{r}(t) = -P_{r}(t)A(t) - A^{T}(t)P_{r}(t) - Q + P_{r}(t)B(t)R^{-1}B^{T}(t)P_{r}(t) \tag{4.9}$$

CHAPTER 5

RESULTS AND DISCUSSIONS

In this chapter, suspension performance in terms of control torque, lateral displacement and yaw angle of the wheelsets including vehicle body acceleration of two-axle railway vehicle are discussed for different inputs; radius of curved track for front and rear wheelset, cant angle of curved track for front and rear wheelset and vehicle velocity.

5.1 Track Input Parameters

5.1.1 Standard Input Values Simulation

The standard input values are presented in Figure 5.1; for cant angle value is 14º while for curve radius value is 1500 m and for vehicle velocity is 60 ms^{-1}. This standard values is the actual parameters used in railway vehicle system.

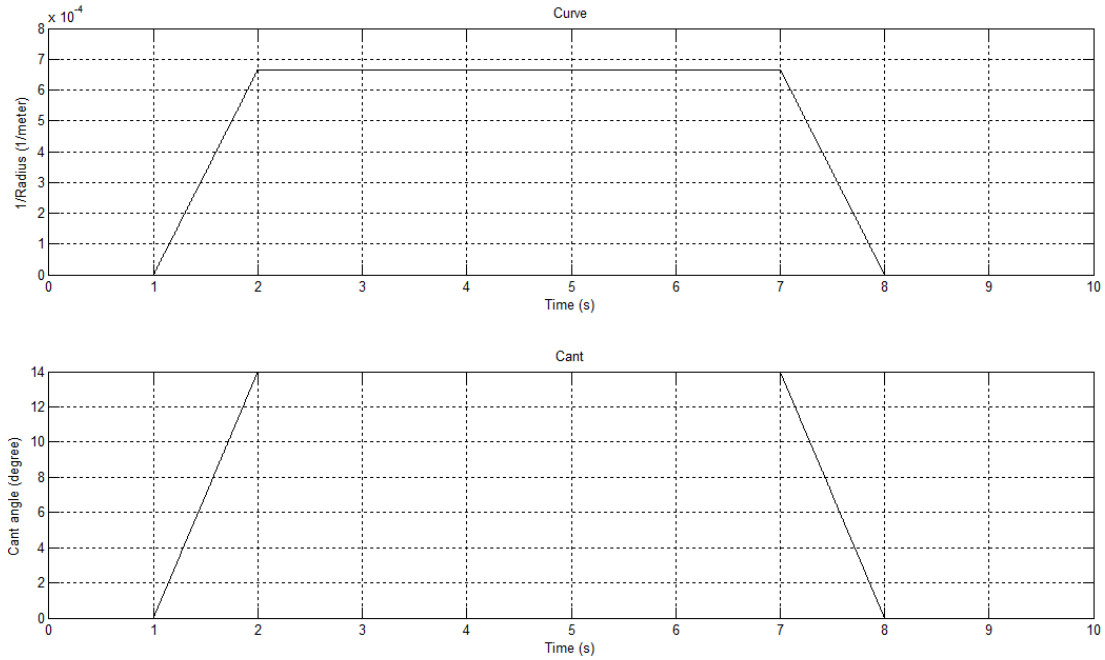

Figure 5.1: Curve Radius (1/meter) and Cant Angle (degree)

Next, for the simulation result; Figure 5.2(a) show that control torque value for standard input value is lower than 200 Nm. During the transition from straight to curved track, the control torque is necessary to provide active damping which stabilizes the wheelset. Figure 5.2(a) shown where the torque vector is in negative direction as the wheelset moves from straight to curved track. When the wheelset leaves the curve, the torque vector changes its direction. The larger control effort is required during curve transition, while smaller and constant control torque during steady curve.

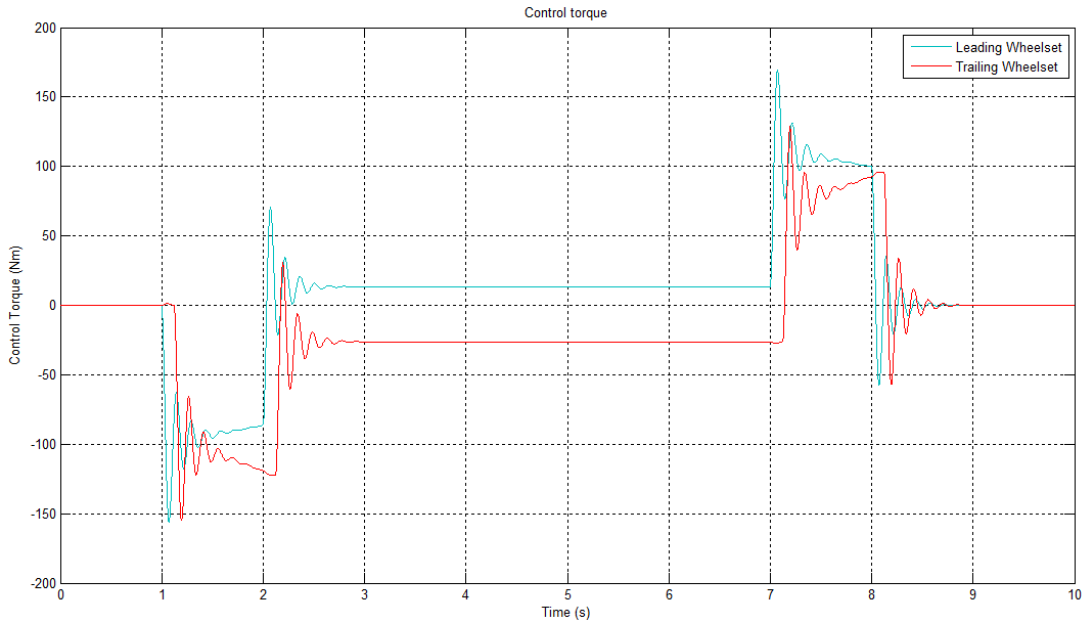

Figure 5.2(a): Control Torque (Nm)

In Figure 5.2(b), it can be seen that, the lateral displacement of the wheelset on the steady curve is 1.1 mm under the given condition. The yaw angle in Figure 5.3(c) increases during curve transition from less than 0.035 mrad. during steady curve.

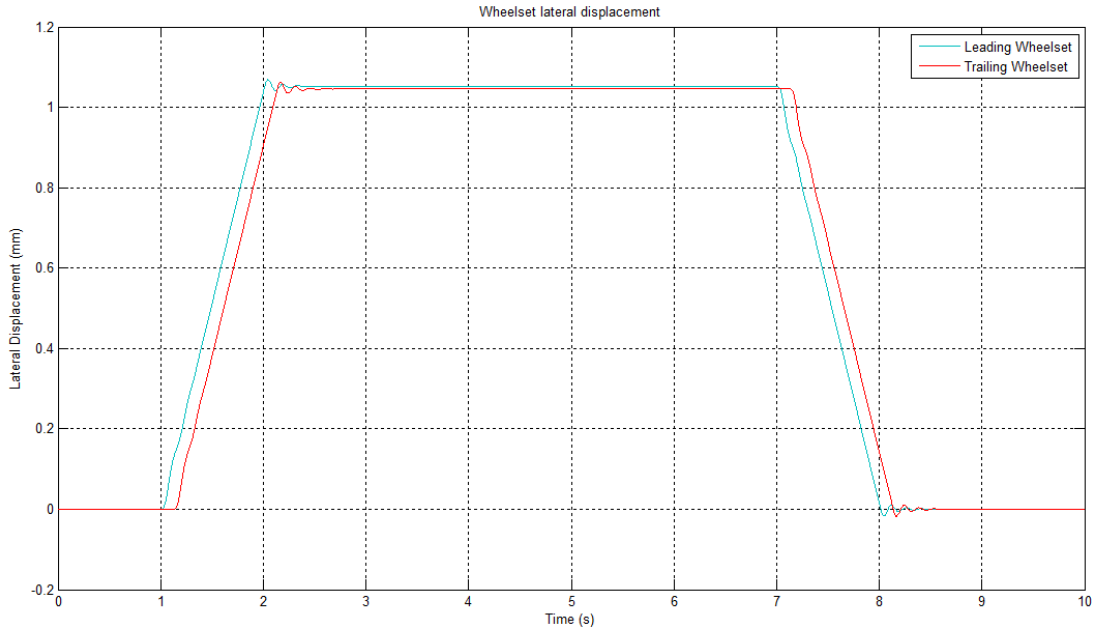

Figure 5.2(b): Wheelset Lateral Displacement (mm)

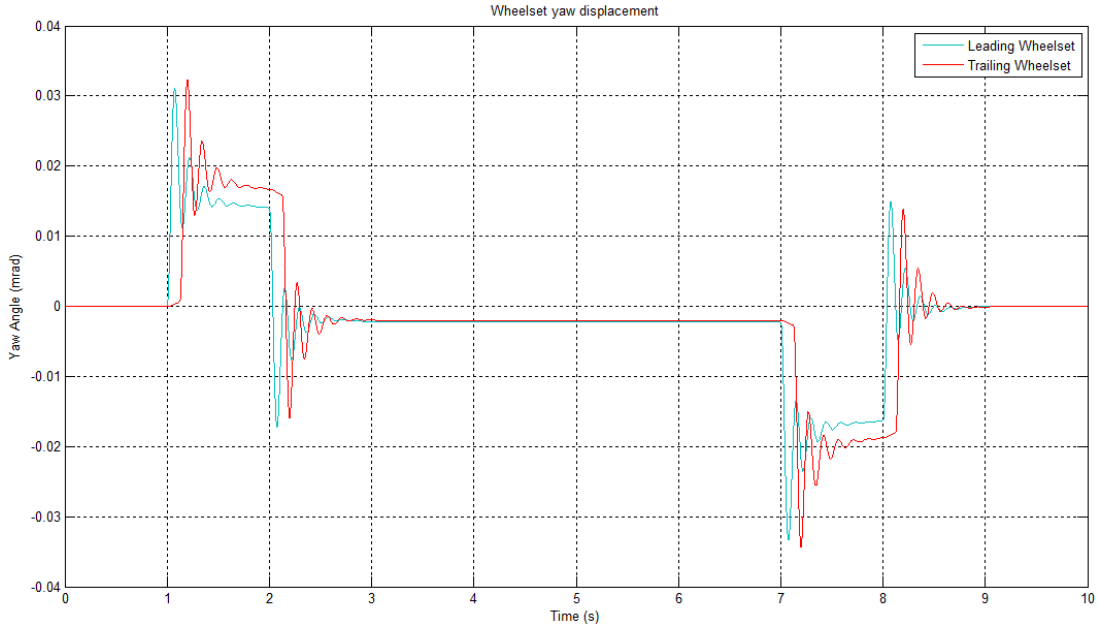

Figure 5.2(c): Wheelset Yaw Displacement (mrad.)

Lastly, for the body lateral acceleration on curve transition for two axle vehicle is 0.08 ms^{-2} (or equal to 0.008 g), which is small, as shown in Figure 5.2(d). At steady curve, the lateral acceleration is equal to zero, meaning that no vibration if the train carrying goods during this moment.

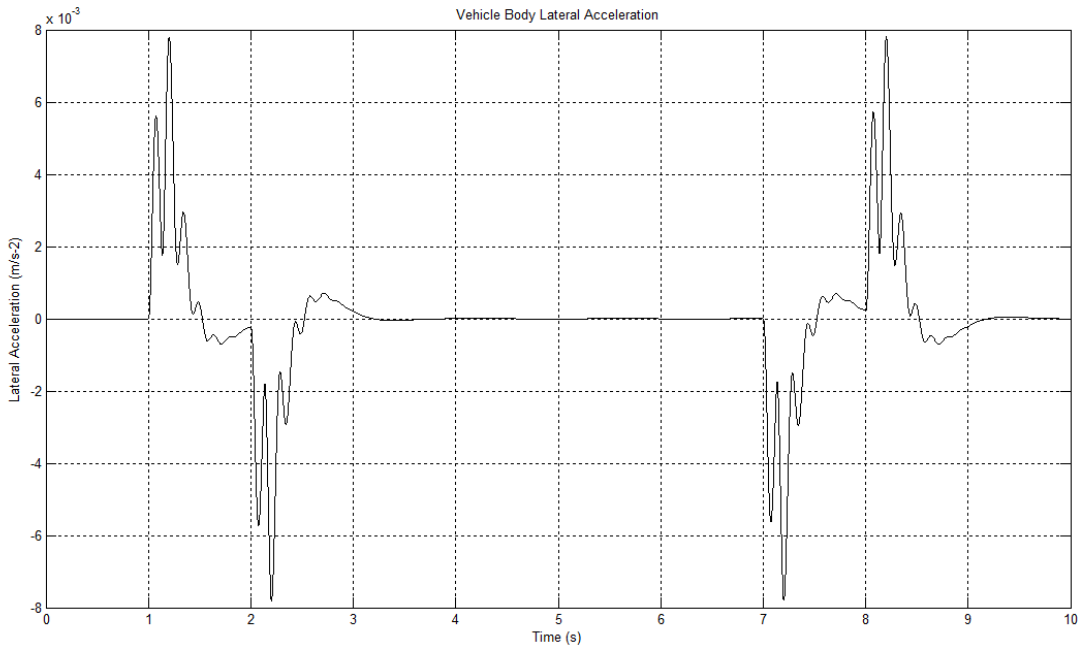

Figure 5.2(d): Vehicle Body Lateral Acceleration (ms^{-2})

5.1.2 Different Input Value Simulation

For this subtopic, as mention in project objective, the different value for input parameters are used to demonstrate the curving performance and vehicle body acceleration. This section will include all graphs of simulations that have done for different input values.

5.1.2.1 Track Input Value

For the next different value simulation, one from the standard values simulation is change while others two standard values are remain; Figure 5.3(a) show the curved radius value is change from 1500 m to 1000 m while Figure 5.3(b) show the curved radius is change from 1500 m to 2000 m. As for Figure 5.3(c) and Figure 5.3(d), the cant angle is change from 14º to 7º and 14º to 21º each. Vehicle velocity input also change which are 60 ms^{-1} to 80 ms^{-1} and 60 ms^{-1} to 100 ms^{-1}, however the graph is not available because the change made in velocity does not display in graph term.

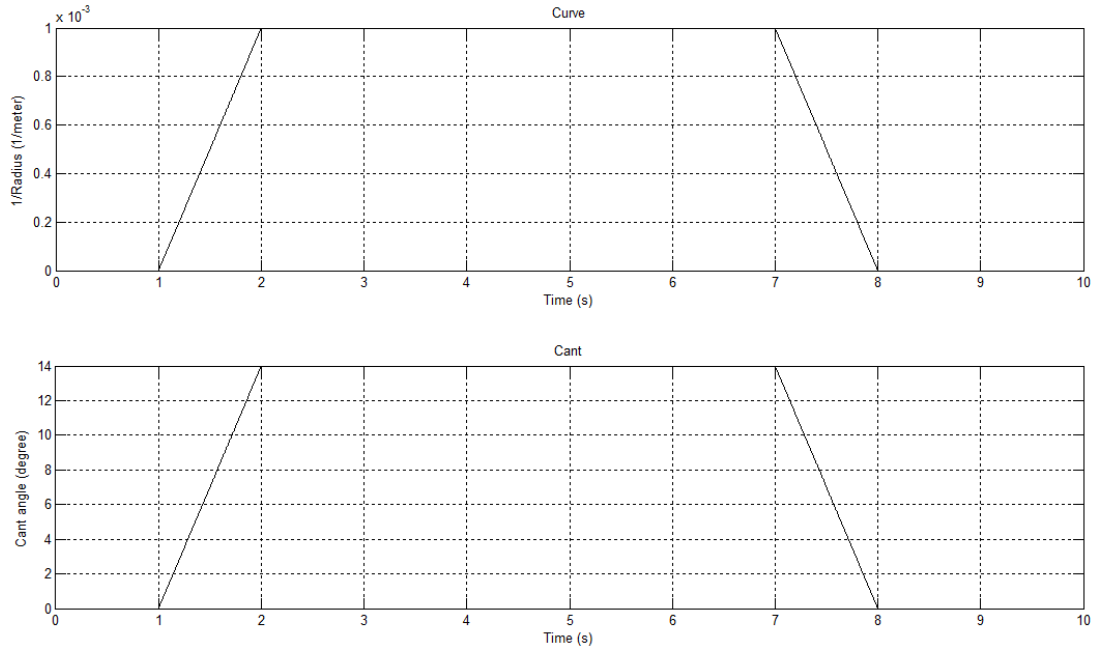

Figure 5.3(a): Curve Radius (1/meter) and Cant Angle (degree) at curved radius 1000 m

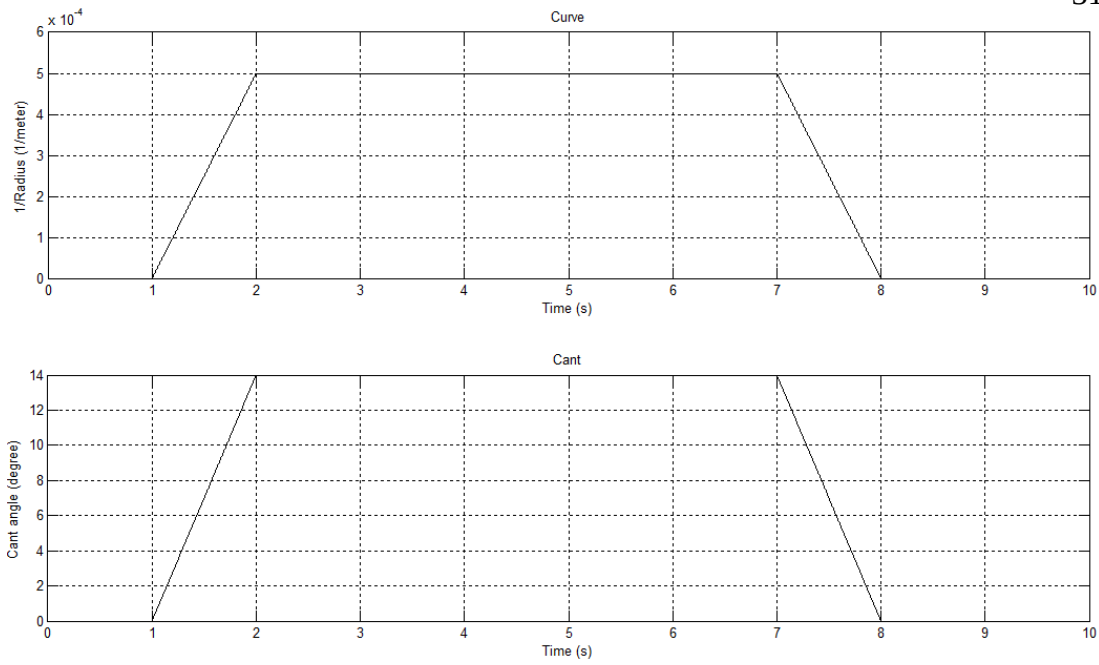

Figure 5.3(b): Curve Radius (1/meter) and Cant Angle (degree) at curved radius 2000 m

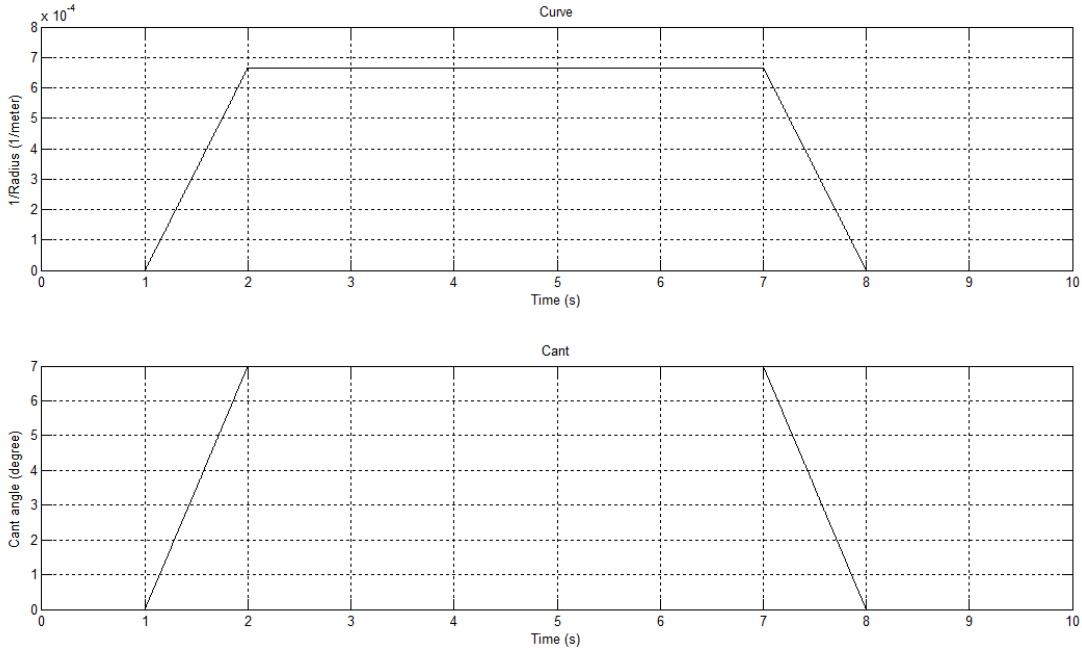

Figure 5.3(c): Curve Radius (1/meter) and Cant Angle (degree) at cant angle 7º

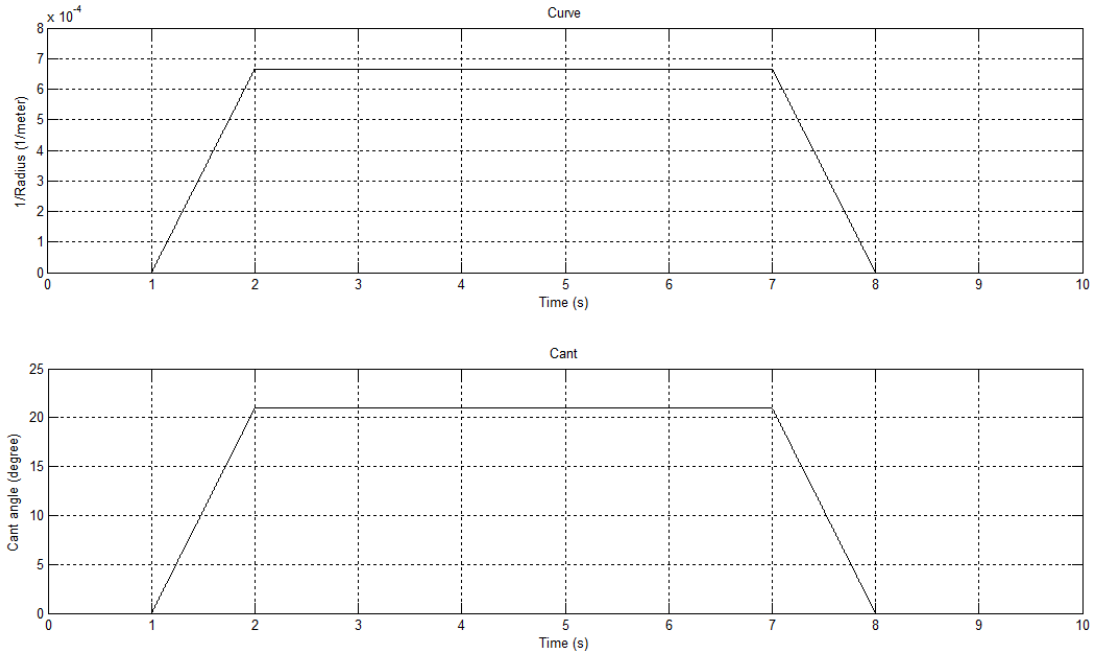

Figure 5.3(d): Curve Radius (1/meter) and Cant Angle (degree)
at cant angle 21°

5.1.2.2 Control Torque Value

According from the input value from subtopic 5.1.2.1, Figure 5.4(a) and Figure 5.4(b) are control torque value for input in Figure 5.3(a) and Figure 5.3(b) each. Also for Figure 5.4(c) and Figure 5.4(d), the input value is from Figure 5.3(c) and Figure 5.3(d) accordingly. Lastly, for Figure 5.4(e) and Figure 5.4(f), the input change is vehicle velocity which are $60ms^{-1}$ to $80ms^{-1}$ and $60ms^{-1}$ to $100ms^{-1}$ each.

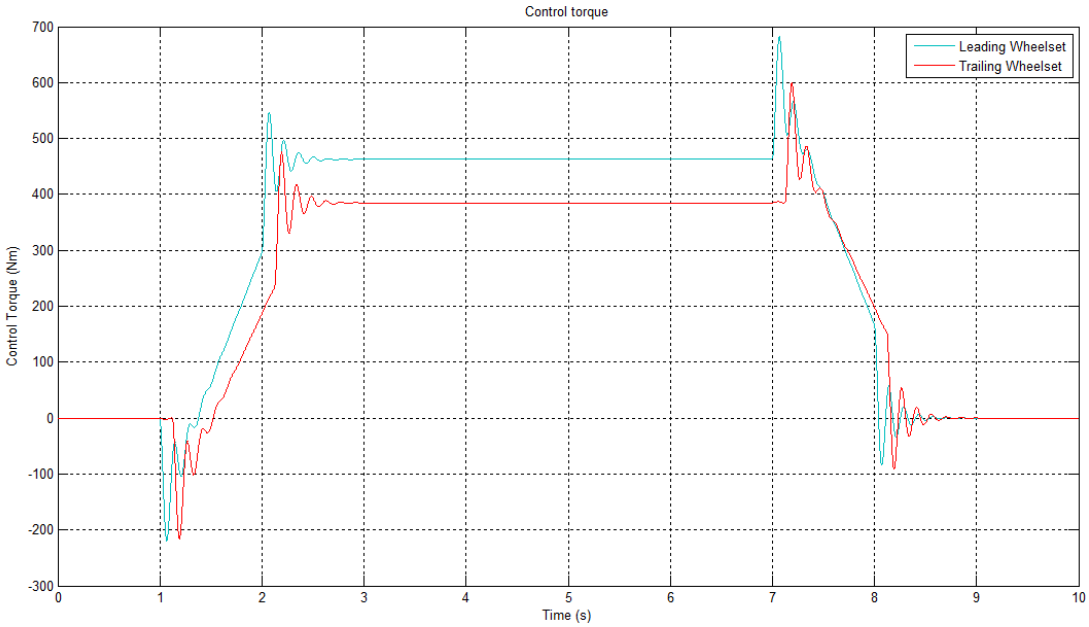

Figure 5.4(a): Control Torque (Nm) at curved radius 1000 m

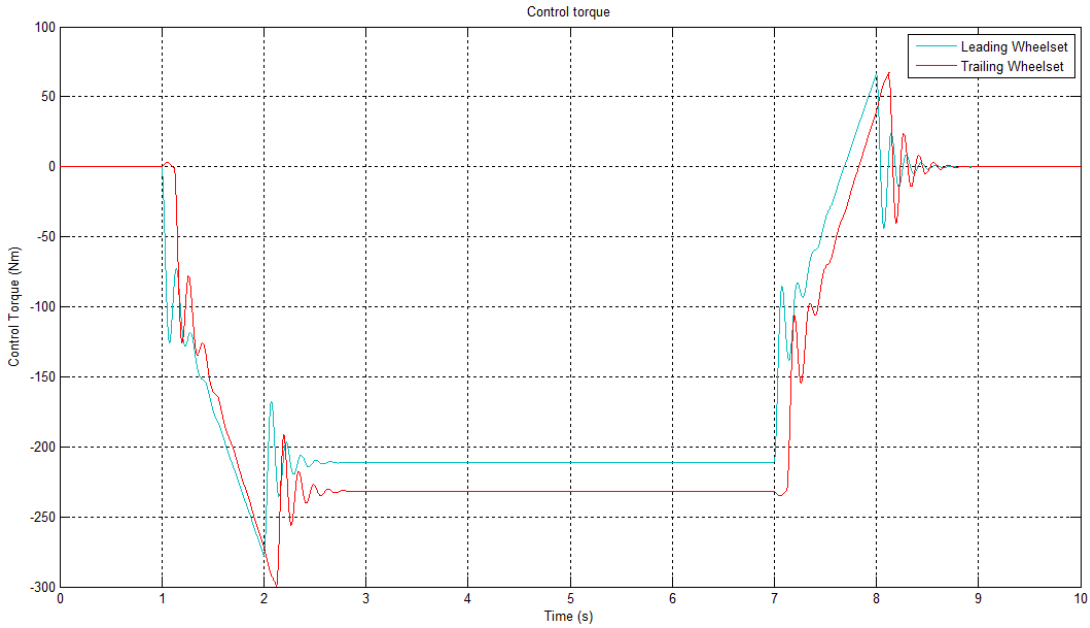

Figure 5.4(b): Control Torque (Nm) at curved radius 2000 m

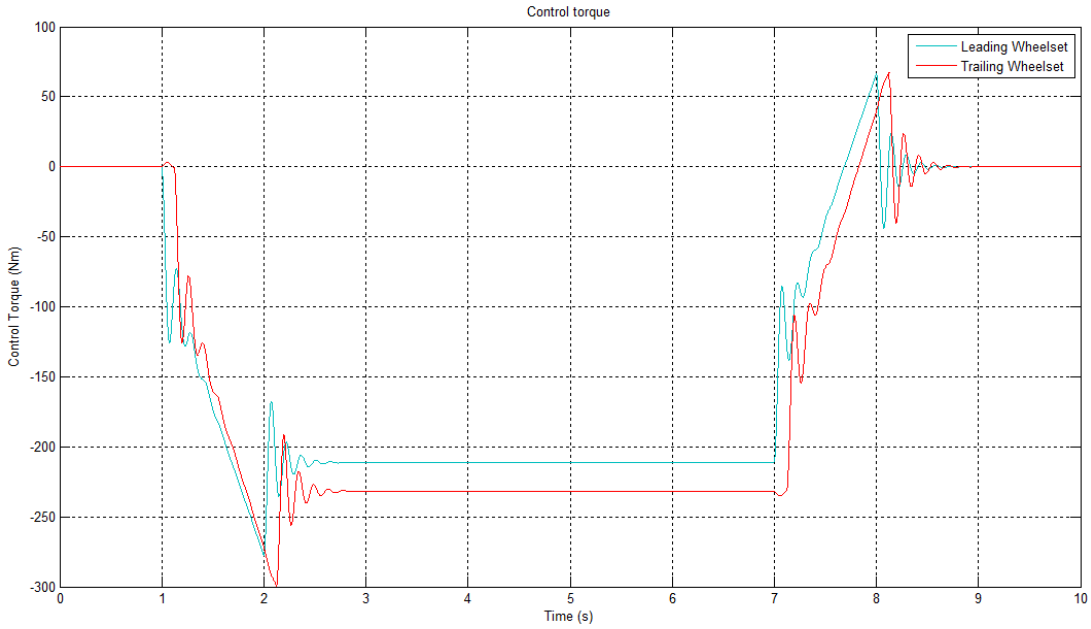

Figure 5.4(c): Control Torque (Nm) at cant angle 7º

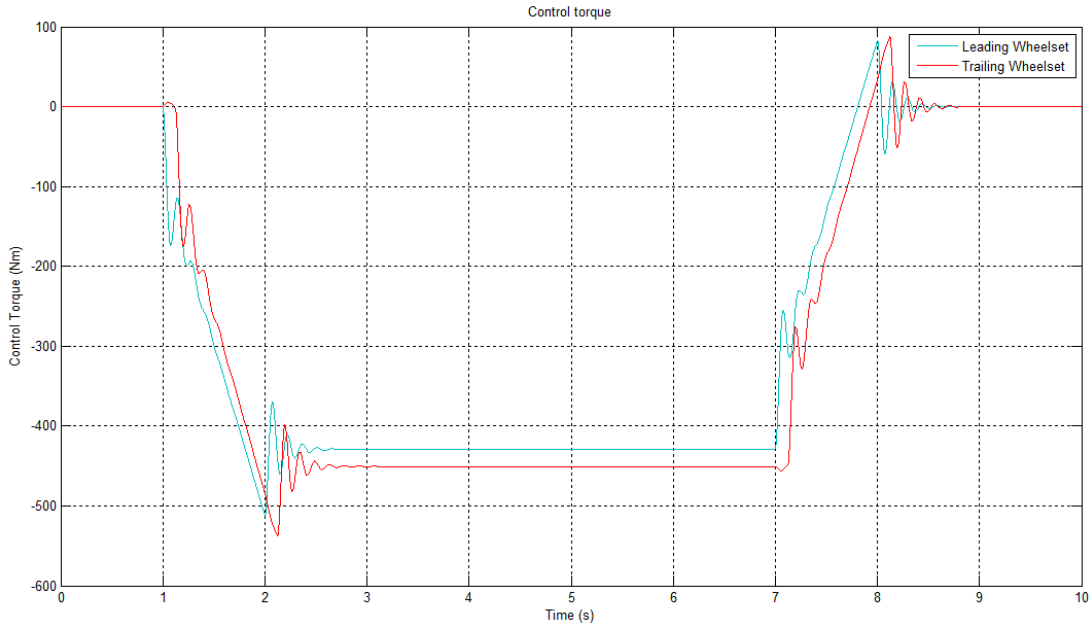

Figure 5.4(d): Control Torque (Nm) at cant angle 21º

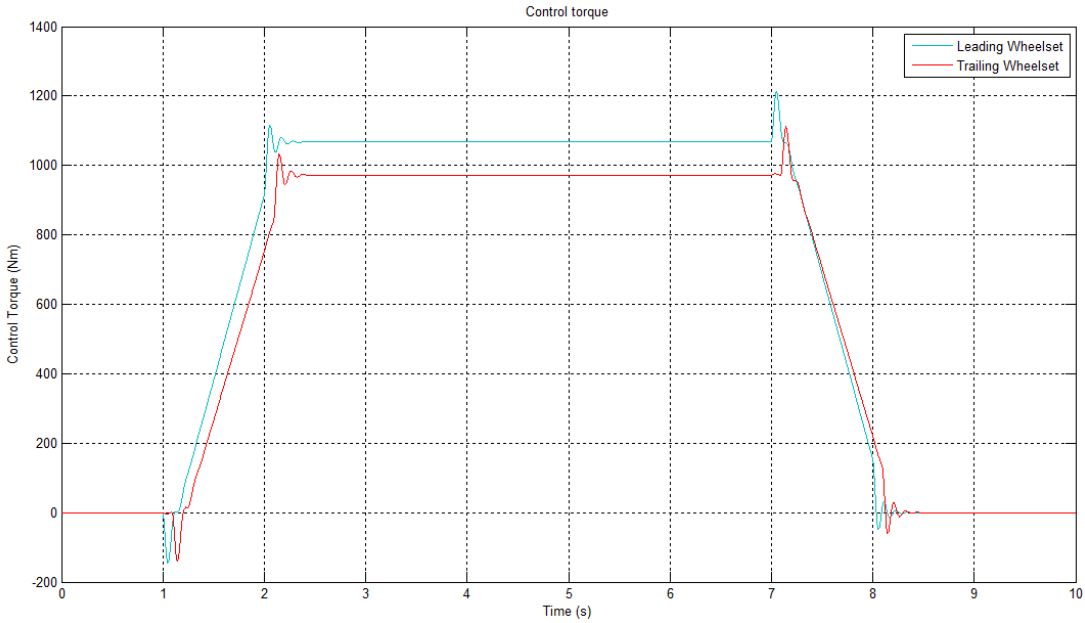

Figure 5.4(e): Control Torque (Nm) at vehicle velocity 80ms^{-1}

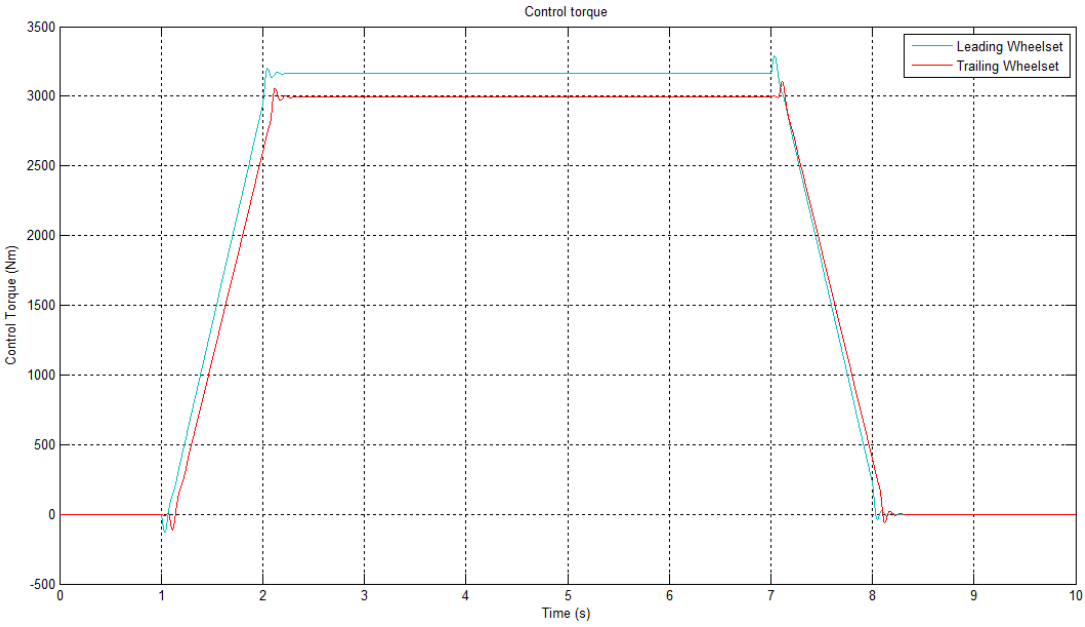

Figure 5.4(f): Control Torque (Nm) at vehicle velocity 100ms^{-1}

5.1.2.3 Wheelset Lateral Displacement Value

According from the input value from subtopic 5.1.2.1, Figure 5.5(a) and Figure 5.5(b) are wheelset lateral displacement value for input in Figure 5.3(a) and Figure 5.3(b) each. Also for Figure 5.5(c) and Figure 5.5(d), the input value is from Figure 5.3(c) and Figure 5.3(d) accordingly. Lastly, for Figure 5.5(e) and Figure 5.5(f), the input change is vehicle velocity which are 60ms^{-1} to 80ms^{-1} and 60ms^{-1} to 100ms^{-1} each.

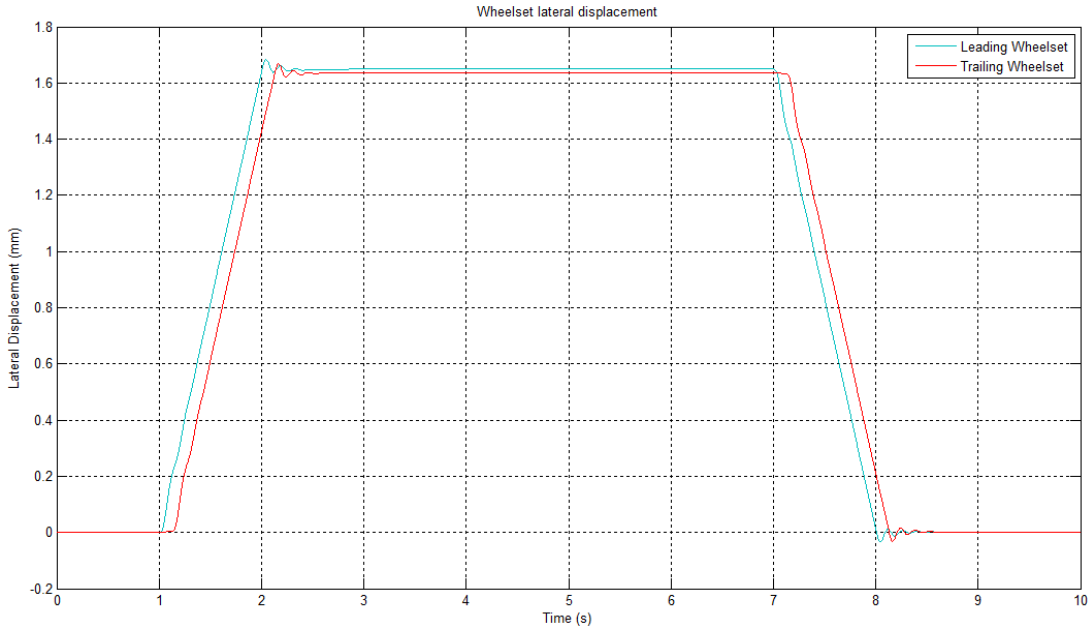

Figure 5.5(a): Wheelset Lateral Displacement (mm) at curved radius 1000 m

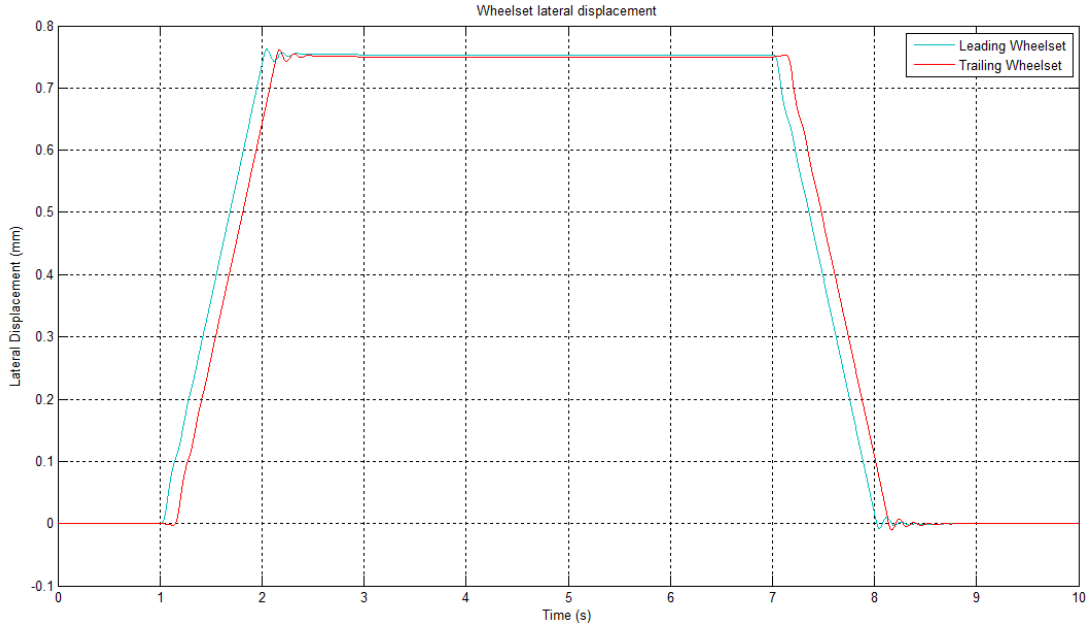

Figure 5.5(b): Wheelset Lateral Displacement (mm) at curved radius 2000 m

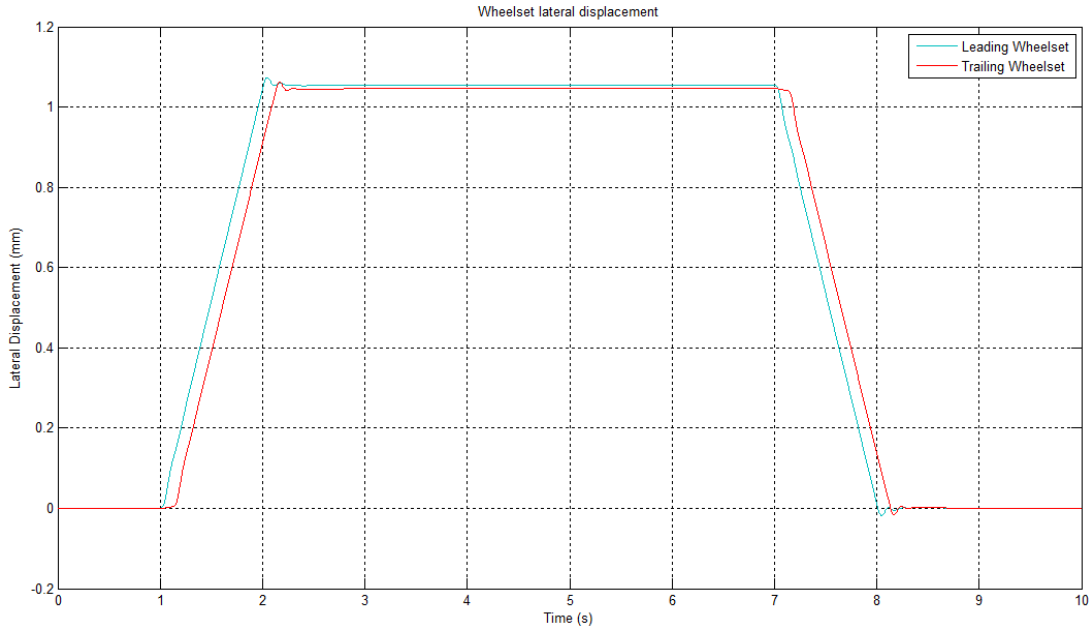

Figure 5.5(c): Wheelset Lateral Displacement (mm) at cant angle 7º

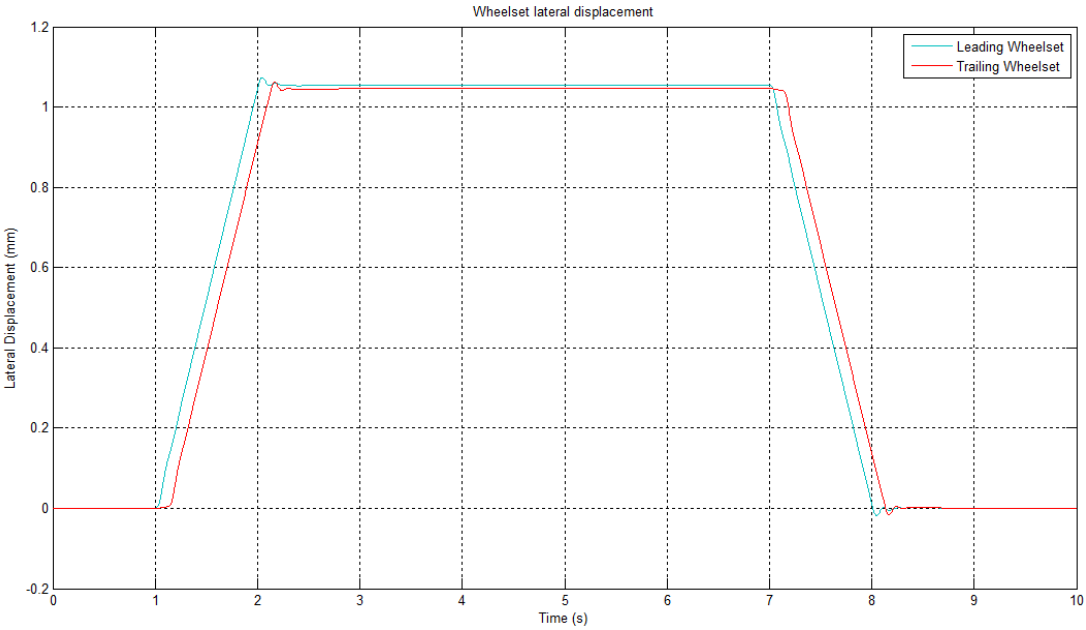

Figure 5.5(d): Wheelset Lateral Displacement (mm) at cant angle 21º

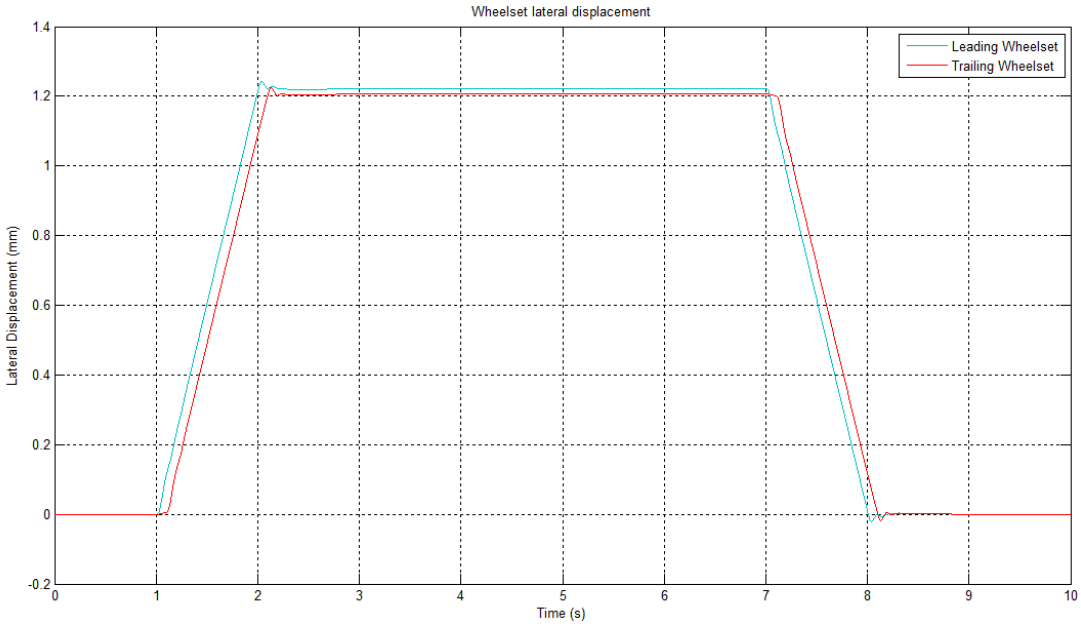

Figure 5.5(e): Wheelset Lateral Displacement (mm) at vehicle velocity 80ms^{-1}

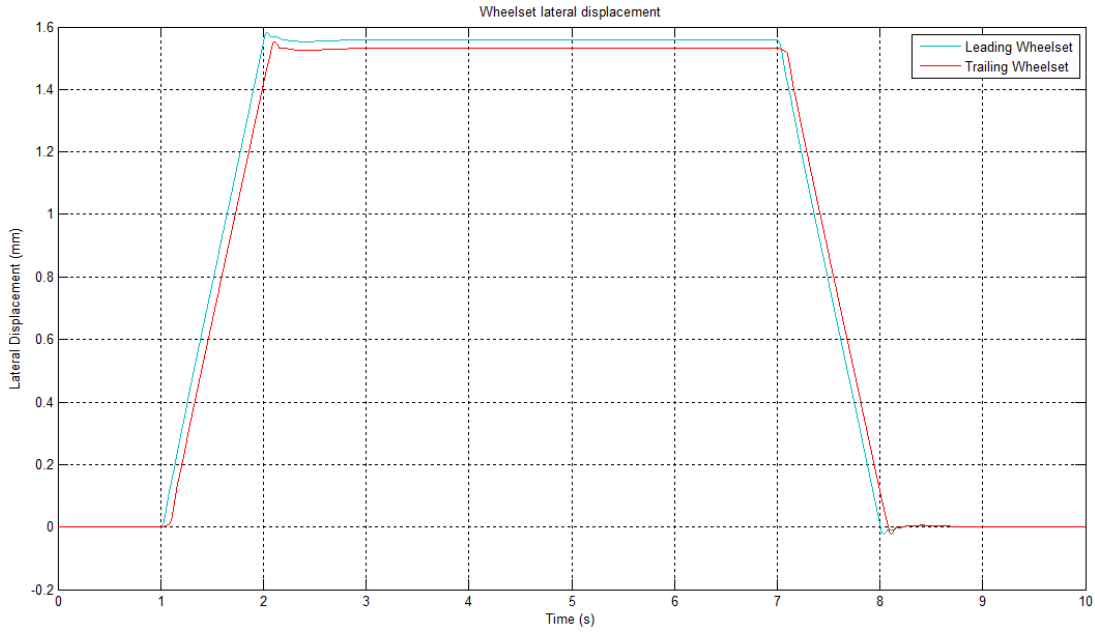

Figure 5.5(e): Wheelset Lateral Displacement (mm) at vehicle velocity 100ms^{-1}

5.1.2.4 Wheelset Yaw Displacement Value

According from the input value from subtopic 5.1.2.1, Figure 5.6(a) and Figure 5.6(b) are wheelset yaw displacement value for input in Figure 5.3(a) and Figure 5.3(b) each. Also for Figure 5.6(c) and Figure 5.6(d), the input value is from Figure 5.3(c) and Figure 5.3(d) accordingly. Lastly, for Figure 5.6(e) and Figure 5.6(f), the input change is vehicle velocity which are 60ms^{-1} to 80ms^{-1} and 60ms^{-1} to 100ms^{-1} each.

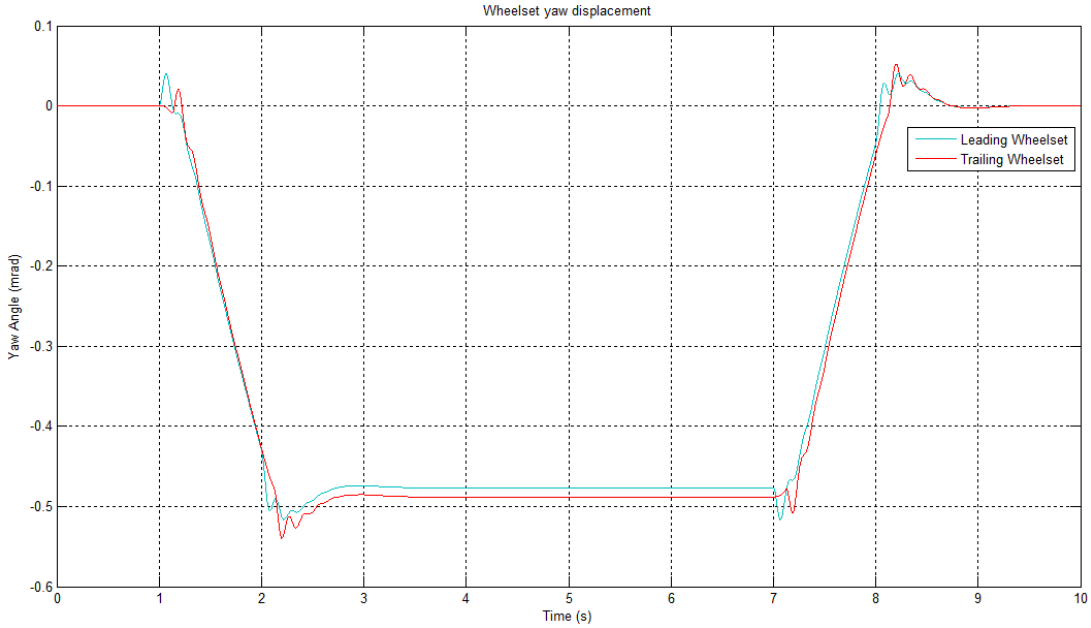

Figure 5.6(a): Wheelset Yaw Displacement (mrad.) at curved radius 1000 m

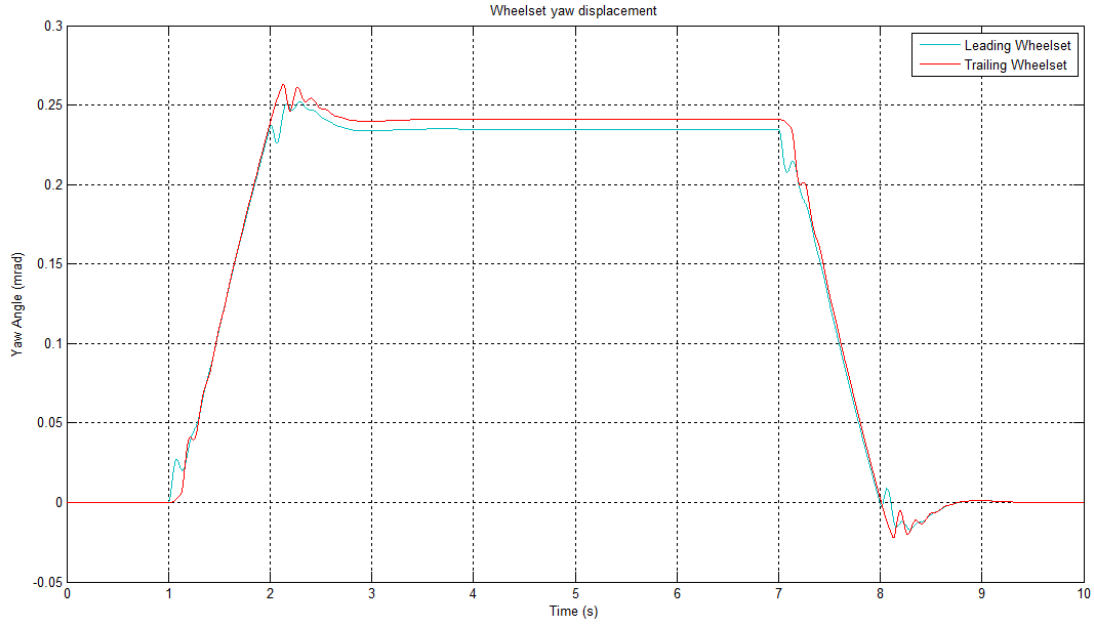

Figure 5.6(b): Wheelset Yaw Displacement (mrad.) at curved radius 2000 m

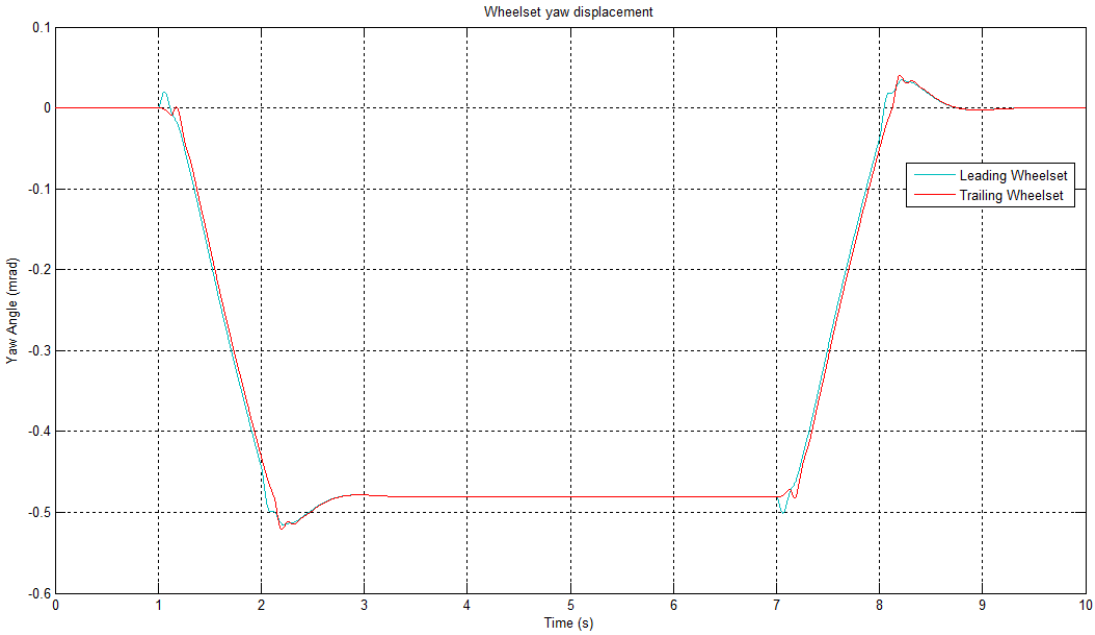

Figure 5.6(c): Wheelset Yaw Displacement (mrad.) at cant angle 7º

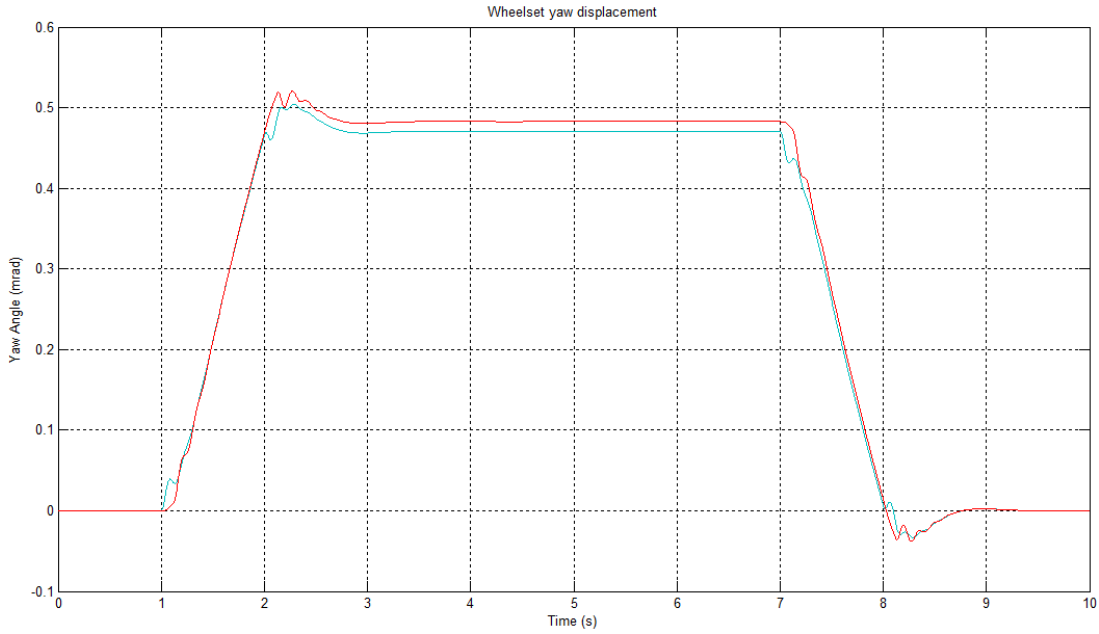

Figure 5.6(d): Wheelset Yaw Displacement (mrad.) at cant angle 21º

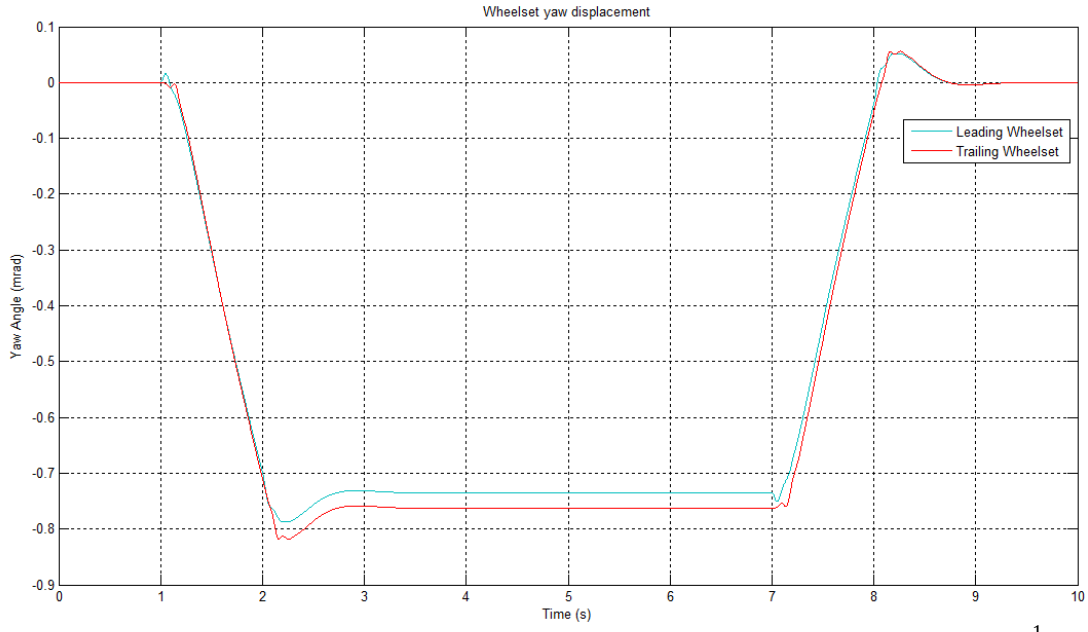

Figure 5.6(e): Wheelset Yaw Displacement (mrad.) at vehicle velocity 80 ms^{-1}

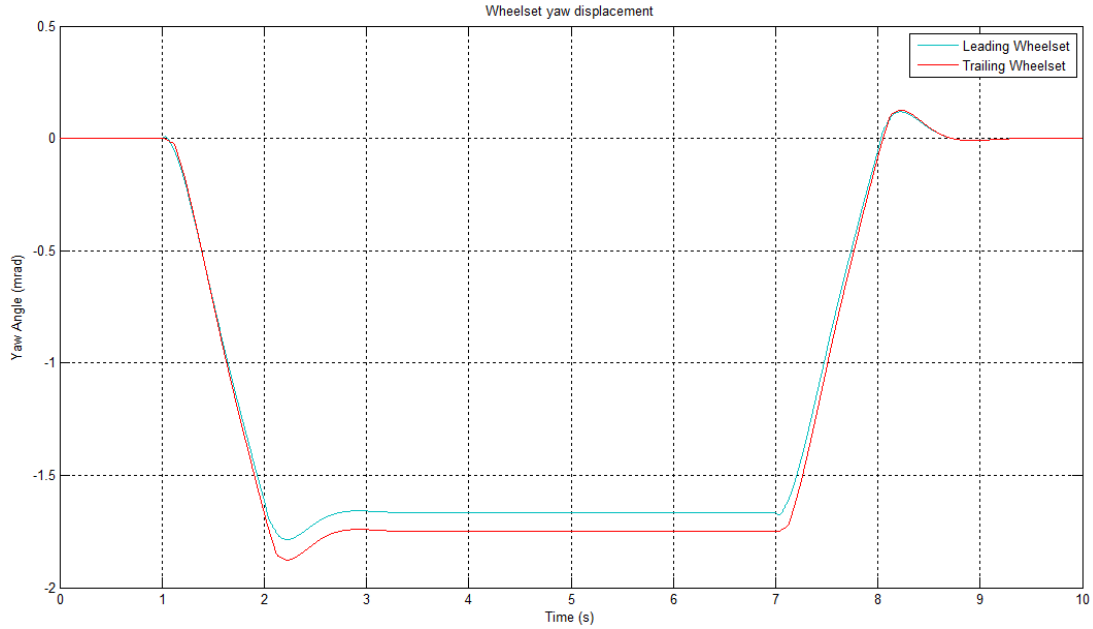

Figure 5.6(f): Wheelset Yaw Displacement (mrad.) at vehicle velocity 100 ms^{-1}

5.1.2.5 Vehicle Body Acceleration Value

According from the input value from subtopic 5.1.2.1, Figure 5.7(a) and Figure 5.7(b) are vehicle body acceleration value for input in Figure 5.3(a) and Figure 5.3(b) each. Also for Figure 5.7(c) and Figure 5.7(d), the input value is from Figure 5.3(c) and Figure 5.3(d) accordingly. Lastly, for Figure 5.7(e) and Figure 5.7(f), the input change is vehicle velocity which are $60ms^{-1}$ to $80ms^{-1}$ and $60ms^{-1}$ to $100ms^{-1}$ each.

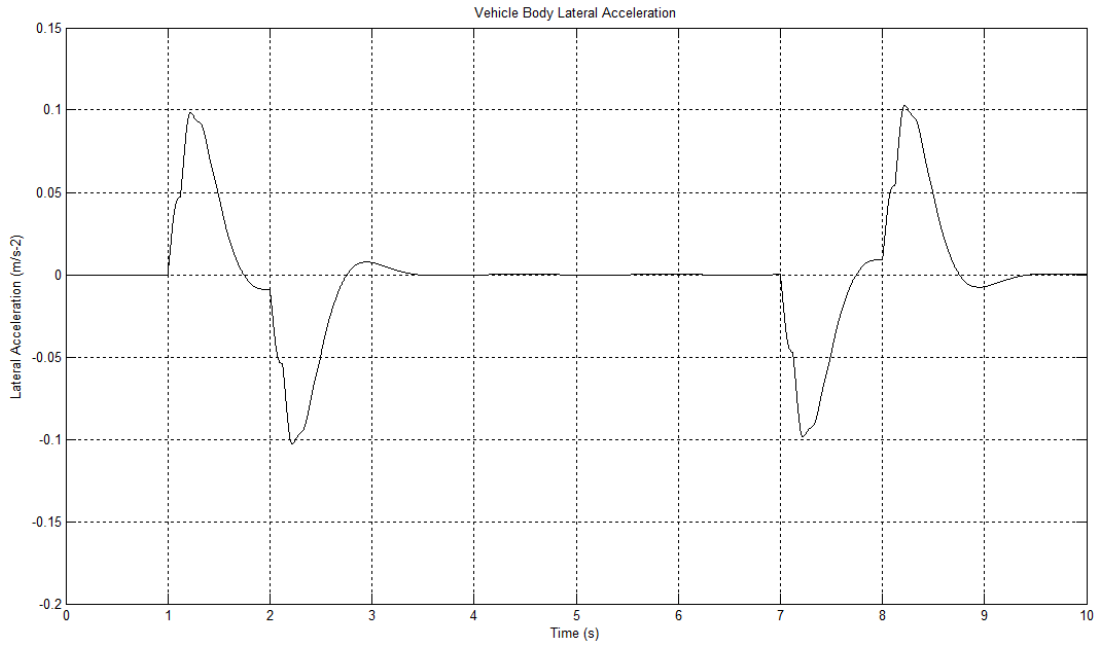

Figure 5.7(a): Vehicle Body Lateral Acceleration at curved radius at 1000 m

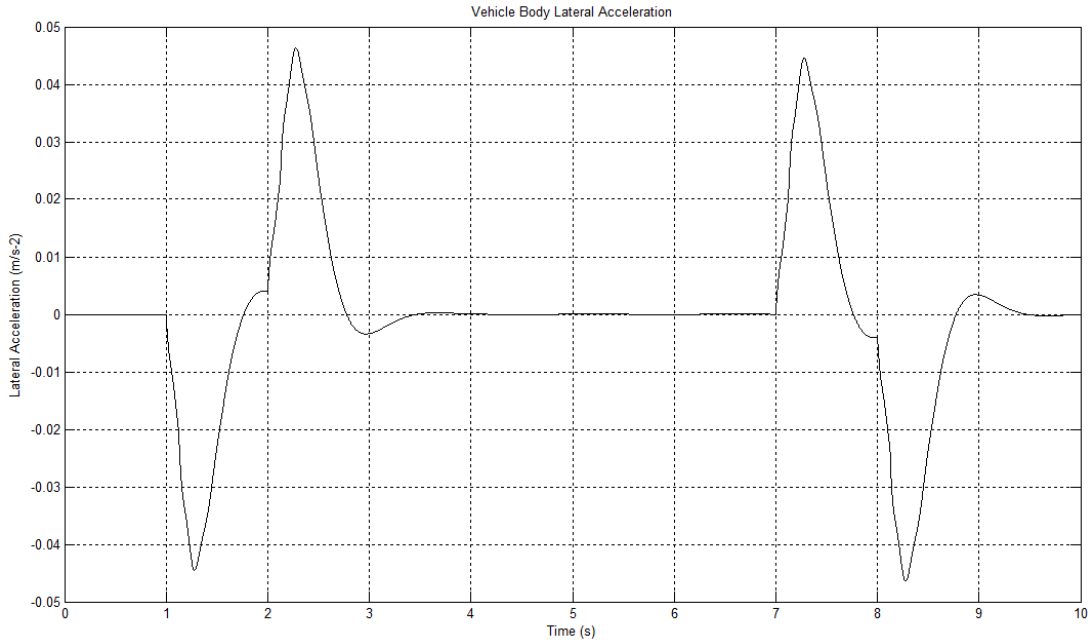

Figure 5.7(b): Vehicle Body Lateral Acceleration at curved radius at 2000 m

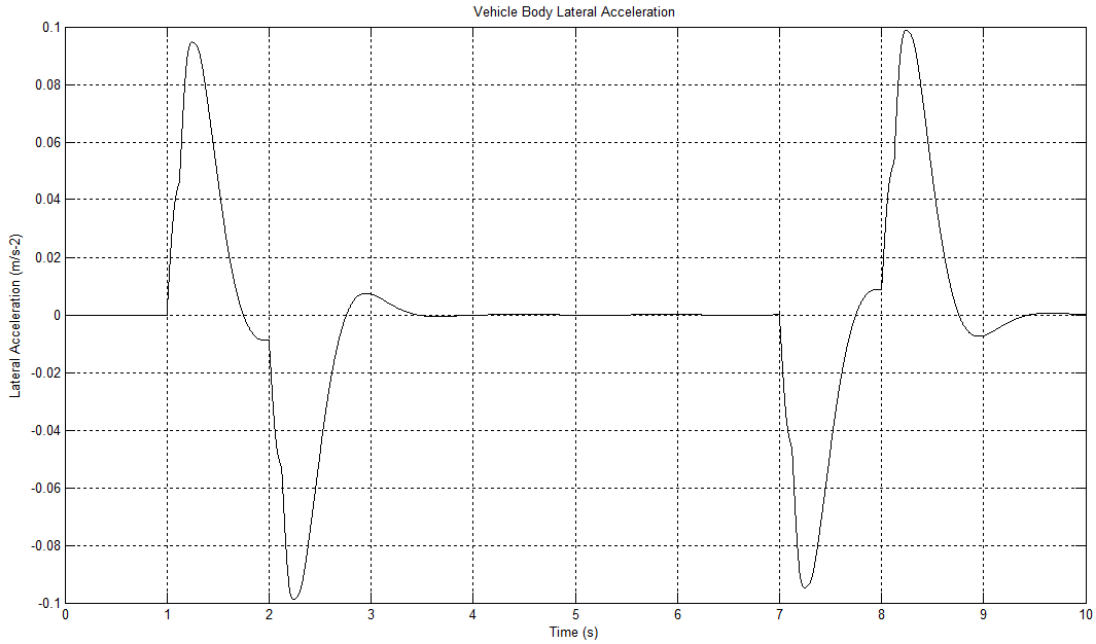

Figure 5.7(c): Vehicle Body Lateral Acceleration at cant angle 7º

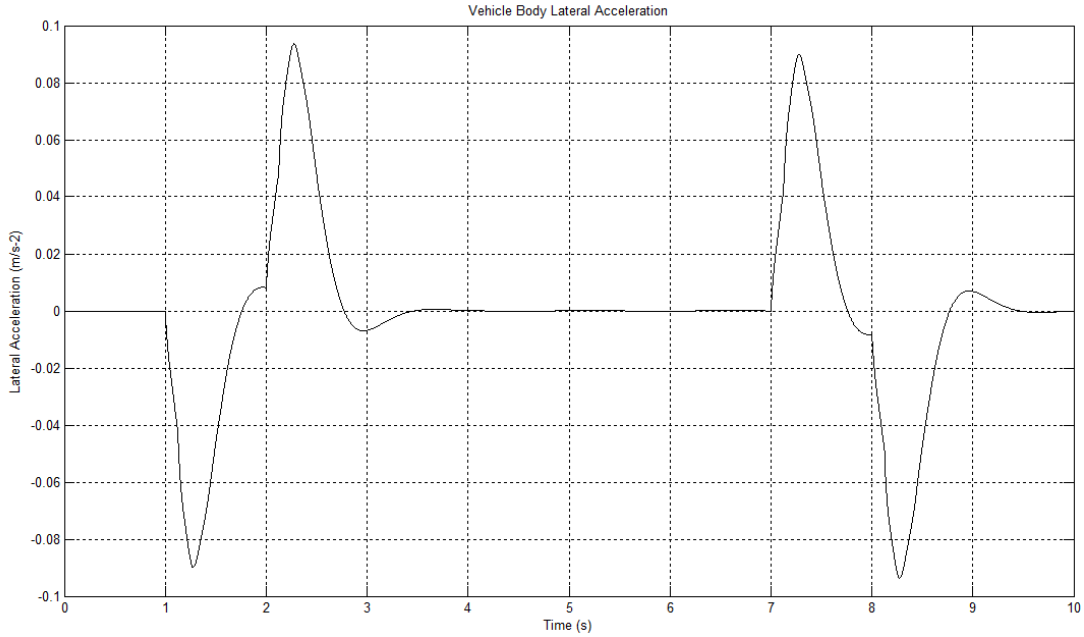

Figure 5.7(d): Vehicle Body Lateral Acceleration at cant angle 21º

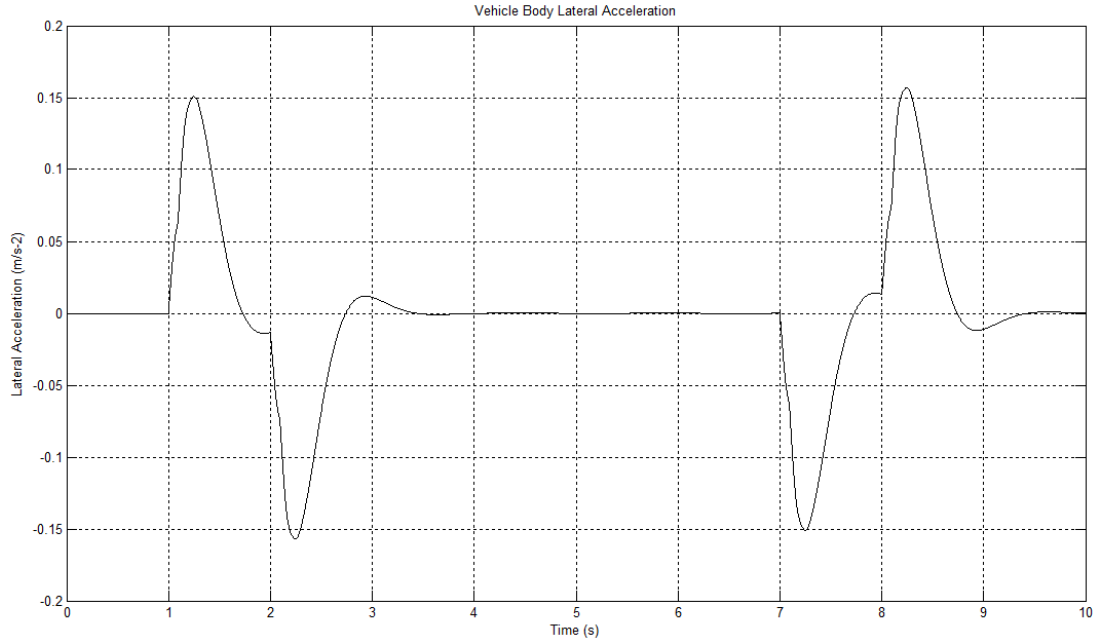

Figure 5.7(e): Vehicle Body Lateral Acceleration at vehicle velocity 80 ms^{-1}

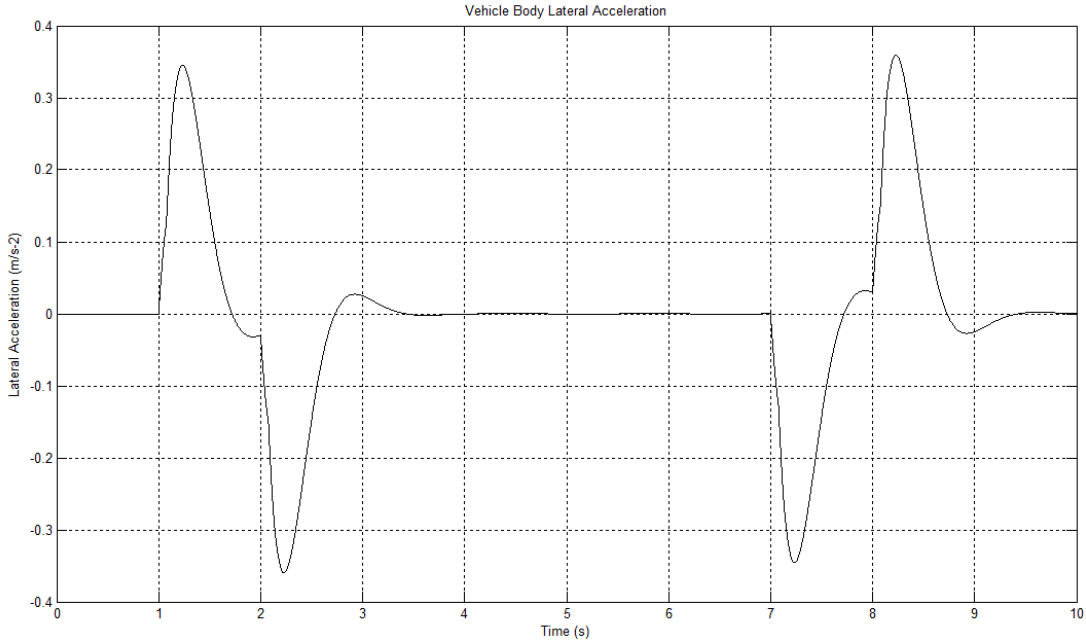

Figure 5.7(f): Vehicle Body Lateral Acceleration at vehicle velocity 100 ms^{-1}

5.2 Summary

In this section, the performances of different values of input are discussed and compared. All the inputs change are capable to give better performance during the curving. However, each output results from different inputs has its own advantages over the others. Standard values are use for this study; curved radius value is 1500 m, cant angle value is 14º and vehicle velocity is 60ms^{-1}.

To simplify the different performance of each inputs change under this study; one from the standard values simulation is change while others two standard values are remain which are R stand for curved radius, V is vehicle velocity and C will be cant angle input, the simulation results for all inputs are listed in the following table:

Table 5.1: Comparison for different inputs

Output value / Input change	Control Torque (Nm)	Wheelset Lateral Displacement (mm)	Wheelset Yaw Displacement (mrad.)	Vehicle Body Acceleration (ms^{-2})
Standard values	≤ 160	1.10	≤ 0.0035	0.079
R=1000m	≤ 690	1.68	≤ 0.5400	0.100
R=2000m	≤ 300	0.76	≤ 0.2530	0.047
C=7º	≤ 220	1.06	≤ 0.5300	0.090
C=21º	≤ 530	0.90	≤ 0.5300	0.093
V=80ms^{-1}	≤ 1220	1.25	≤ 0.8200	0.152
V=100ms^{-1}	≤ 3300	1.59	≤ 1.8900	0.360

CHAPTER 6

CONCLUSION AND RECOMMENDATIONS

6.1 Conclusion

This thesis has studied the optimal control for active steering of a two-axle vehicle with the solid axle wheelset. It has demonstrated that, for all input that applied have own advantages. For example; the wheelset lateral displacement for curved radius equal to 2000 m is 0.76 mm; the value is better than standard input because of smaller lateral displacement in wheelset but the value was measured in mili then it will not effect the wheelset performance.

In this study, the standard value have the better performance than other values and become the better choice to be choose as the value for the input. The values of weighting matrices for optimal control are crucial and careful selection is needed to get a good curving performance for each input values.One major disadvantage of optimal control is the requirement of full state feedback which is not practical and economic. Alternatively, it is highly desirable to design other control structures that do not require the full state feedback.

6.2 Future Recommendation

For future study or research, several improvements can be made to the results. The suggestions are listed as follow:

(i) Different types of modern control technique are implemented into the active suspension railway vehicle system to overcome the limitations of optimal control and comparison between two different types of controller used.

(ii) Design a new dynamic model and simulate the curving performance and stability with another type of wheelset arrangements with bogie or independant rotating wheelset (IRW).

(iii) Develop a test rig and hardware that can collect experimental results and compared with simulation results.

REFERENCES

[1] Goodall, R. M. and Kortum, W. Active Controls in Ground Transportation. *Vehicle System Dynamics*. 1983; Vol. 12: 227.

[2] Raman K. Mehra, Jayesh N. Amin, Karl J. Hendrick, Carlos Osario and Srinivasan Gopalasamy, *Active Suspension Using Preview Information and Model Predictive Control*, SBIR Pahse I and US Army, 5-7 October 1997, Page 860 – 861.

[3] Y.M. Sam and J.H.S. Osman (UTM), M.R.A. Ghani (KUTKM), *Active Suspension Control: Performance Comparison using Proportional Integral Sliding Mode and Linear Quadratic Regulator Methods*, IEEE Xplore, Page 274.

[4] Piet, M. and Broersen, T. Stability and Riding Quality of railway Vehicles. *Vehicle System Dynamics*. 1974; Vol. 3: 113.

[5] Mei, T. X. Perez, J. and Goodall R. M. Design of optimal PI control for perfect curving of railway vehicles with solid-axle wheelsets. *UKACC Int. Conf. on Control 2000*. Cambridge, UK. 2000.

[6] Peterson, G. R. Superelevation and Transition Spiral Primer. 2004. pp. 2.

[7] Rail Safety and Standards Board. Track System Requirement: *Track gauge*. London. Apr. 2007.

[8] Kufver, B. and Forstberg, J. Tracks for Tilting Trains: *Fast and Comfortable Trains*. European Commision. Aug. 2004.

[9] T.X Mei, Z. Nagy, R.M Goodall, and A.H *Wickens, Mechatronic solutions for high-speed railway vehicles*, Elsevier Science Ltd., 26 October 2001, Page 1023 – 1028.

[10] Wikipedia (2009), Linear Quadratic Regulator
URL http://en.wikipedia.org/wiki/Linear-quadratic_regulator

[11] William L. Brogan, "Modern control theory", 3rd ed., Englewood Cliffs, N.J., Prentice Hall, 1991.

[12] F. L. Lewis (1999). “EE 4343/5329 - Control System Design Project”.

[13] Goodall, R. M. Tilting trains and beyond: The future for active railway suspensions. *Computing & Control Engineering Journal*. Oct 1999; 222.

[14] Mei, T. X. and Goodall, R. M. Optimal control strategies for active steering of railway vehicles. *Proc. IFAC 1999*. Beijing, China. 1999. 215-256.

[15] Goodall, R. M. Tilting trains and beyond: The future for active railway suspensions. *Computing & Control Engineering Journal*. Aug. 1999; 154.

[16] Bryson, A. E. and Ho, Y. C. *Applied Optimal Control*. Waltham, Massachusetts. Blaidshell Publishing Co. 1969.

APPENDIX A: M-FILE FOR ACTIVE SUSPENSION CONTROL OF TWO AXLE RAILWAY VEHICLE MODELING

```
clc;
clear all;
%defining global variables
global A B G uin w;

%Wheelset parameters
v=60;                    %wheelset forward speed (m/s)
mass=1250;               %wheelset mass (kg)
I=700;                   %yaw inertia (kg m^2)
ro=0.45;                 %wheel radius (m)
length=0.7;              %half gauge of wheelset (m)

Kl=230e3;                %lateral stiffness per wheelset (N/m)
Cl=50e3;                 %lateral damping per wheelset (Ns/m)

c_1=0.2;                 %conicity values  (0.05-0.5)
f_1=10e6;                %creep coefficient (N)

%Secondary mass parameters (half vehicle body)
Mb= 13500;  %30000;       %mass of vehicle body (kg)
Ib= 170000; %558800;    %Yaw inertia of vehicle (kg m^2)
Lb= 3.7; %4.5;           %half-space of vehicle (m)


%State-space matrices of wheelset system
B=[0 0;
0 0;
1/I 0; %1/I
0 0;
0 0;
0 0;
0 1/I; %%1/I
0 0;
0 0;
0 0;
-1/Ib -1/Ib; % -1/Ib  -1/Ib
0 0];

C=[0 1 0 0 0 0 0 0 0 0 0 0 ;   %wheelset 1 lateral displacement
0 0 0 0 0 1 0 0 0 0 0 0 ];  %wheelset 2 lateral displacement

C_yaw=[0 0 0 1 0 0 0 0 0 0 0 0 ;   %wheelset 1 yaw displacement
 0 0 0 0 0 0 0 1 0 0 0 0 ];  %wheelset 2 yaw displacement

D=[0 0;0 0];

A_1=[-2*f_1/(mass*v)-Cl/mass -Kl/mass 0 2*f_1/mass 0 0 0 0
Cl/mass Kl/mass Cl*Lb/mass Kl*Lb/mass ;
```

```
1 0 0 0 0 0 0 0 0 0 0 ;
 0 -2*f_1*length*c_1/(I*ro) -2*f_1*length^2/(I*v) 0 0 0 0 0 0 0 0
 0 ; %a33 -ve
0 0 1 0 0 0 0 0 0 0 0 ;
 0 0 0 0 -2*f_1/(mass*v)-Cl/mass -Kl/mass 0 2*f_1/mass Cl/mass
 Kl/mass -Cl*Lb/mass -Kl*Lb/mass ;
0 0 0 0 1 0 0 0 0 0 0 ;
 0 0 0 0 0 -2*f_1*length*c_1/(I*ro) -2*f_1*length^2/(I*v) 0 0 0 0
 0 ; %a77 -ve
0 0 0 0 0 0 1 0 0 0 0 ;
Cl/Mb Kl/Mb 0 0 Cl/Mb Kl/Mb 0 0 -2*Cl/Mb -2*Kl/Mb 0 0 ;
0 0 0 0 0 0 0 0 1 0 0 ;
 Cl*Lb/Ib Kl*Lb/Ib 0 0 -Cl*Lb/Ib -Kl*Lb/Ib 0 0 0 0 -2*Cl*Lb^2/Ib -
 2*Kl*Lb^2/Ib ;
0 0 0 0 0 0 0 0 0 0 1 0 ];

 B_ctrl=B(1:12,:);

 C_ctrl=[0 1 0 0 0 0 0 0 0 0 0 0;
   0 0 0 1 0 0 0 0 0 0 0 0;
   0 0 0 0 0 1 0 0 0 0 0 0;
   0 0 0 0 0 0 0 1 0 0 0 0];

 D_ctrl=zeros(4,2);
 sys1=ss(A_1(1:12,1:12),B_ctrl,C_ctrl,D_ctrl);

 %Weighting matrices for controller's cost function
 Q=diag([100 10 100 10]*0.001);
 %[100 10 100 10]*0.08 for cant angle = 7o
 %[100 10 100 10]*0.001 for cant angle = 14o
 R=diag([1e-12 1e-12]); %e-12

 %Simulation parameters
 f_sample=400;
 sample=1/f_sample;
 end_time=10;
 end_sim=end_time*f_sample;
 t_change=1;
 N_recalc=f_sample;
 [gain,sol,eigen] = lqry(sys1,Q,R);

 %Track parameters
 g=9.8;
 Radius=1500;
 d=14*pi/180;

 curve=0;
 cant=0;


 %Initialisation
 x0=zeros(12,1);
 u0=zeros(2,1);

 %Managing delayed disturbance at two wheelsets
```

```
Ldiff=2*Lb;                     %distance between two wheelsets
t_delay=Ldiff/v;                %delay between two wheelsets (in
sec.)
delay=t_delay*f_sample;         %delay between two wheelsets (no
unit)

%Generating curve and cant data
s_tran_sec1=1.0;
e_tran_sec1=2.0;
s_tran_sec2=7.0;
e_tran_sec2=8.0;

s_tran1=s_tran_sec1*f_sample;
e_tran1=e_tran_sec1*f_sample;
s_tran2=s_tran_sec2*f_sample;
e_tran2=e_tran_sec2*f_sample;

for i=1:end_sim
if i>s_tran1 & i<e_tran1
  curve=((1/Radius)/(e_tran1-s_tran1))*(i-s_tran1);
  cant=(d/(e_tran1-s_tran1))*(i-s_tran1);
 elseif i>s_tran2 & i<e_tran2
  curve=((1/Radius)/(s_tran2-e_tran2))*(i-e_tran2);
  cant=(d/(s_tran2-e_tran2))*(i-e_tran2);
elseif i>=e_tran1 & i<=s_tran2
  curve=1/Radius;
  cant=d;
else
  curve=0;
  cant=0;
end
curve_data(:,i)=[curve(:)];
cant_data(:,i)=[cant(:)];
end



%START OF SIMULATION

for t=1:end_sim
time=(t-1)/f_sample;
%error=[noisef(2,t);noiser(2,t)];

yt_dot_f= 0 ; %track_vel(t);
curve_f=curve_data(t);%0
cant_f=cant_data(t);%0
t_rear=round(t-delay);

if t_rear<1
 yt_dot_r=0;
 curve_r=0;
 cant_r=0;
else
 yt_dot_r= 0; %track_vel(t_rear);
 curve_r=curve_data(t_rear);%
```

```
 cant_r=cant_data(t_rear);%
end


w=[curve_f;cant_f;yt_dot_f;curve_r;cant_r;yt_dot_r];



%Wheelset model

A=[-2*f_1/(mass*v)-Cl/mass -Kl/mass 0 2*f_1/mass 0 0 0 0 Cl/mass
Kl/mass Cl*Lb/mass Kl*Lb/mass ;
1 0 0 0 0 0 0 0 0 0 0 0 ;
 0 -2*f_1*length*c_1/(I*ro) -2*f_1*length^2/(I*v) 0 0 0 0 0 0 0 0
0 ; %a33 -ve
0 0 1 0 0 0 0 0 0 0 0 0 ;
 0 0 0 0 -2*f_1/(mass*v)-Cl/mass -Kl/mass 0 2*f_1/mass Cl/mass
Kl/mass -Cl*Lb/mass -Kl*Lb/mass ;
0 0 0 0 1 0 0 0 0 0 0 0 ;
 0 0 0 0 0 -2*f_1*length*c_1/(I*ro) -2*f_1*length^2/(I*v) 0 0 0 0
0 ; %a77 -ve
0 0 0 0 0 0 1 0 0 0 0 0 ;
Cl/Mb Kl/Mb 0 0 Cl/Mb Kl/Mb 0 0 -2*Cl/Mb -2*Kl/Mb 0 0 ;
0 0 0 0 0 0 0 0 1 0 0 0 ;
 Cl*Lb/Ib Kl*Lb/Ib 0 0 -Cl*Lb/Ib -Kl*Lb/Ib 0 0 0 0 -2*Cl*Lb^2/Ib
-2*Kl*Lb^2/Ib ;
0 0 0 0 0 0 0 0 0 0 1 0 ];



%Track disturbance matrix
G=[v^2 -g 0 0 0 0; %g12 -ve
 0 0 -1 0 0 0;
 2*f_1*length^2/I 0 0 0 0 0;
 0 0 0 0 0 0;
 0 0 0 v^2 -g 0; %g55 -ve
 0 0 0 0 0 -1;
 0 0 0 2*f_1*length^2/I 0 0;
 0 0 0 0 0 0;
 v^2/2 -g/2 0 v^2/2 -g/2 0;
 0 0 -1/2 0 0 -1/2;
 0 0 0 0 0 0;
 0 0 0 0 0 0];

%Simulate wheelset model
x=x0;
uin=u0;
u(:,t)=[uin(:)];
[tout,xout]=ode45('train',[time time+sample],x);
[row,col]=size(xout);
x0=xout(row,:)';
xt(:,t)=[x(:)];
yout=C*x0; %+error;
y(:,t)=[yout(:)];
zout=C_yaw*x0; %+error;
z(:,t)=[zout(:)];
```

```
%Control signal generation
   A_ctrl=[-2*f_1/(mass*v)-Cl/mass -Kl/mass 0 2*f_1/mass 0 0 0 0
Cl/mass Kl/mass Cl*Lb/mass Kl*Lb/mass ;
     1 0 0 0 0 0 0 0 0 0 0 0 ;
 0 -2*f_1*length*c_1/(I*ro) -2*f_1*length^2/(I*v) 0 0 0 0 0 0 0 0
0 ; %a33 -ve
     0 0 1 0 0 0 0 0 0 0 0 0 ;
 0 0 0 0 -2*f_1/(mass*v)-Cl/mass -Kl/mass 0 2*f_1/mass Cl/mass
Kl/mass -Cl*Lb/mass -Kl*Lb/mass ;
     0 0 0 0 1 0 0 0 0 0 0 0 ;
 0 0 0 0 0 -2*f_1*length*c_1/(I*ro) -2*f_1*length^2/(I*v) 0 0 0 0
0 ; %a77 -ve
     0 0 0 0 0 0 1 0 0 0 0 0 ;
     Cl/Mb Kl/Mb 0 0 Cl/Mb Kl/Mb 0 0 -2*Cl/Mb -2*Kl/Mb 0 0 ;
     0 0 0 0 0 0 0 0 1 0 0 0 ;
 Cl*Lb/Ib Kl*Lb/Ib 0 0 -Cl*Lb/Ib -Kl*Lb/Ib 0 0 0 0 -2*Cl*Lb^2/Ib
-2*Kl*Lb^2/Ib ;
     0 0 0 0 0 0 0 0 0 0 1 0 ];


sys=ss(A_ctrl(1:12,1:12),B_ctrl,C_ctrl,D_ctrl);

 [gain,sol,eigen] = lqry(sys,Q,R);
 u0=-gain*x0(1:12);

u_data(:,t)=[u0(:)];

gain_data(:,t)=[gain(:)];

acc(:,t)=A(9,:)*x0(:)+B(9,:)*u0(:)+G(9,:)*w(:);
end



%%%%%%%%%%%%%%%%%%%%%%%%%%%%%%%%%%%%
%%%%%%% PERFORMANCE PLOTS %%%%%%%%
%%%%%%%%%%%%%%%%%%%%%%%%%%%%%%%%%%%%
p=sample:sample:end_time;

figure(1)
subplot(2,1,1);
plot(p,curve_data,'k');
ylabel('1/Radius (1/meter)');
xlabel('Time (s)');
grid;
title('Curve')
subplot(2,1,2);
%figure(2)
plot(p,cant_data/pi*180,'k');
ylabel('Cant angle (degree)');
xlabel('Time (s)');
grid;
title('Cant');
```

```
figure(3)
plot(p,u_data,'k');
ylabel('Control Torque (Nm)');
xlabel('Time (s)');
grid;
title('Control torque');

figure(4)
plot(p,y*1e3,'k');
ylabel('Lateral Displacement (mm)');
xlabel('Time (s)');
grid;
title('Wheelset lateral displacement');

figure(5)
plot(p,z*1e3,'k');
ylabel('Yaw Angle (mrad)');
xlabel('Time (s)');
grid;
title('Wheelset yaw displacement');

figure(6)
plot(p,acc,'k');
ylabel('Lateral Acceleration (m/s-2)');
xlabel('Time (s)');
grid;
title('Vehicle Body Lateral Acceleration');
```